OAK RIDGE
NATIONAL LABORATORY

MANAGED BY UT-BATTELLE
FOR THE DEPARTMENT OF ENERGY

ORNL/TM-2000/97

A New Method to Determine the Thermal Properties of Soil Formations from In Situ Field Tests

J. A. Shonder
J. V. Beck

UT-BATTELLE

ORNL-27 (4-00)

ORNL/TM-2000/97

A New Method to Determine the Thermal Properties of Soil Formations from In Situ Field Tests

J. A. Shonder
Energy Division, Oak Ridge National Laboratory

J. V. Beck
Professor Emeritus, Michigan State University

April 2000

Prepared by
OAK RIDGE NATIONAL LABORATORY
Oak Ridge, Tennessee 37831-6285
managed by
UT-BATTELLE, LLC
for the
U.S. DEPARTMENT OF ENERGY
under contract DE-AC05-00OR22725

CONTENTS

List of Figures and Tables v
Acknowledgments vii
Abbreviations and Symbols ix

1. INTRODUCTION 1-1
2. A NEW METHOD FOR DETERMINING SOIL THERMAL PROPERTIES 2-1
   2.1 Introduction 2-1
   2.2 The Physical Problem 2-2
   2.3 Energy Fluid Model 2-3
   2.4 Energy Model for Soil, Grout, and Film 2-4
   2.5 The GPM Software 2-8
   2.6 Conclusions 2-8
3. FIELD TESTS OF THE GPM SOFTWARE 3-1
   3.1 Field Rig Tests 3-1
   3.2 In Situ Tests at Two Elementary Schools 3-3
      3.2.1 Description of Tests 3-4
      3.2.2 Test Results 3-7
      3.2.3 Comparison with Other Analysis Techniques 3-9
   3.3 Conclusions 3-13
4. GPM SOFTWARE TUTORIAL 4-1
   4.1 Introduction 4-1
   4.2 Main Menu 4-1
   4.3 Output Window 4-5
5. CONCLUSIONS 5-1
6. REFERENCES 6-1

FIGURES AND TABLES

Figures

2.1 Geometry of borehole heat exchanger 2-2
2.2 Control volume for thermal analysis of borehole heat exchanger 2-3
3.1 Measured and predicted average water temperature for experiment using the Oklahoma State University test rig 3-2
3.2 Residuals for the experiment on the Oklahoma State University test rig 3-2
3.3 Sequential estimates of sand and grout thermal conductivity 3-4
3.4 Power input and average water temperature, Campbell Elementary School test #1 3-5
3.5 Power input and average water temperature, Campbell Elementary School test #2 3-6
3.6 Power input and average water temperature, Maxey Elementary School test #1 3-6
3.7 Model error for Campbell Elementary School test #1 3-7
3.8 Model error for Campbell Elementary School test #2 3-8
3.9 Model error for Maxey Elementary School test #1 3-8
3.10 Sequential thermal conductivity estimates, Campbell Elementary School test #1 3-11
3.11 Sequential thermal conductivity estimates, Campbell Elementary School test #2 3-11
3.12 Sequential thermal conductivity estimates, Maxey Elementary School test #1 3-12
3.13 Temperature and power input vs time for a case in which the generator developed mechanical problems 3-12
3.14 Sequential thermal conductivity estimates from the data of Fig. 3.13 3-13
4.1 The main data input screen in GPM 4-1
4.2 A sample of the file dialog box 4-2
4.3 Cross-sectional view of borehole showing dimensions 4-4
4.4 The GPM output window 4-5

Tables

3.1 Parameters of three in situ thermal properties tests performed at Lincoln, Nebraska, elementary schools 3-5
3.2 Results of soil thermal conductivity and borehole resistance estimates from three in situ tests 3-9
3.3 Thermal conductivity estimates derived by three test methods from 50-h tests 3-9

ACKNOWLEDGMENTS

The authors would like to express their appreciation to the following individuals and institutions for their support and collaboration in this work: Lew Pratsch of the U.S. Department of Energy; Larry Hennings, Tim Pratt, Patrick Decker, Julie Kleager, and Brent Adams of the Lincoln Public School District; Dr. Marvin Smith and Dr. Jeffrey Spitler of Oklahoma State University; and Dr. Cenk Yavuzturk of the University of Wyoming.

ABBREVIATIONS AND SYMBOLS

Abbreviations

BHEx	borehole heat exchanger
Btu	British thermal unit
cfm	cubic feet per minute
CV	constant volume
diam	diameter
EMS	energy management system
GHP	geothermal heat pump
GPM	Geothermal Properties Measurement (software)
h	hour
HVAC	heating, ventilating, and air-conditioning
ORNL	Oak Ridge National Laboratory
rms	root mean square
TMY	typical meteorological year
VAV	variable air volume

Variables and Constants

a	radius of U-tube pipe
b	radius of effective pipe
c_p	specific heat
k	thermal conductivity
L	borehole length
$\dot{m}$	flow rate
q'	rate of heat flow per unit length
q''	rate of heat flow per unit area
$\hat{q}_0$	rate at which heat is added to the fluid
r	radial variable
r_0	borehole radius
t	time
T	temperature
$\overline{T}$	average temperature
$\hat{T}$	measured temperature
x	axial variable
α	thermal diffusivity
δ	film thickness
ρ	density
ρc_p	volumetric heat capacity

Subscripts

c	cold or outlet side
h	hot or inlet side
i	time increment i
s	soil
g	grout
ϕ	thin film
∞	infinity

1. INTRODUCTION

The geothermal or ground-source heat pump (GHP) has been shown to be a very efficient method of providing heating and cooling for buildings. GHPs exchange (reject or extract) heat with the earth by way of circulating water, rather than by use of circulating outdoor air, as with an air-source heat pump. The temperature of water entering a GHP is generally cooler than that of outdoor air when space cooling is required, and warmer than that of outdoor air when space heating is required. Consequently, the temperature lift across a GHP is less than the lift across an air-source heat pump. The lower temperature lift leads to greater efficiency, higher capacity at extreme outdoor air temperatures, and better indoor humidity control. These benefits are achieved, however, at the cost of installing a ground heat exchanger. In general, this cost is proportional to length of the heat exchanger, and for this reason there is an incentive to install the minimum possible length such that design criteria are met.

The design of a ground heat exchanger for a GHP system requires, at a minimum, the operating characteristics of the heat pumps, estimates of annual and peak block loads for the building, and information about the properties of the heat exchanger: the size of the U-tubes, the grouting material, etc. The design also requires some knowledge of the thermal properties of the soil, namely thermal conductivity, thermal diffusivity, and undisturbed soil temperature. In the case of a vertical borehole heat exchanger (BHEx) these properties generally vary with depth; therefore, in the design, effective or average thermal properties over the length of the borehole are usually sought. When the cost of doing so can be justified, these properties are measured in an in situ experiment: a test well is drilled to a depth on the same order as the expected depth of the heat pump heat exchangers; a U-tube heat exchanger is inserted and the borehole is grouted according to applicable state and local regulations; water is heated and pumped through the U-tube (using a field generator to power the equipment, or line voltage where available); and the inlet and outlet water temperatures are measured as a function of time. Data on inlet and outlet temperature, power input to the heater and pump, and water flow rate are collected at regular intervals — typically 1 to 15 min — for the duration of the experiment, which may be as long as 60 h.

Two common methods for determining soil thermal properties from such measurements are the line source method (Morgensen 1983) and the cylinder source method (Kavanaugh and Rafferty 1997). Both are based on long-term approximate solutions to the classical heat conduction problem of an infinitely long heat source in an infinite homogeneous medium. Although there are some differences in the way the two methods are implemented, the only difference between the two models is whether the heat source is considered to be a line or a cylinder. In both methods, power input to the water loop is assumed to be constant.

The simplicity of these methods makes them attractive, but they also have some disadvantages. First of all, because the line source and cylinder source approximations are inaccurate for early time behavior, some of the initial data from the field test must be discarded. The amount of data discarded can affect the property measurement. Also, both methods assume that the heat transfer to the ground loop is constant. In practice, heat input to the loop may vary significantly over the course of a field test due to rough operation of the generator or short-term sags and swells in power line voltage. Presumably, this variation affects the accuracy of the thermal property measurement, but error analysis is rarely performed.

This report presents a new method for determining thermal properties from short-term in situ tests using a parameter estimation technique. Because it is based on numerical solutions to the heat conduction equation, the new method is not affected by short-term variations in heat input. Also,

since the model is accurate even for short times, there is no need to discard initial data. The parameter estimation technique used to determine the properties is based on statistical principles that provide quantitative estimates of measurement accuracy.

The parameter estimation method has now been tested with a laboratory test rig at Oklahoma State University and in field tests at two elementary schools in Lincoln, Nebraska. Using our estimation algorithms, and building on the validation achieved during testing, we have developed a computer program, the Geothermal Properties Measurement (GPM) model, that allows users to determine thermal properties from short-term in situ field tests. This program is currently available free of charge.

In Chapter 2 of this report, we describe the parameter estimation method and discuss the theory behind this method. Chapter 3 describes the test rig experiment and the field tests to validate the method. Chapter 4 provides a tutorial for the GPM software.

2. A NEW METHOD FOR DETERMINING SOIL THERMAL PROPERTIES

2.1 INTRODUCTION

As noted in Chapter 1, two common methods for determining soil thermal properties from in situ field tests are the line source method and the cylinder source method. Both are based on analytical solutions to the classical heat conduction problem of an infinitely long heat source in an infinite homogeneous medium.

The line source method is based on classical theory, according to which, at sufficiently large times, the ground heat exchanger can be modeled as a line heat source in an infinite medium (Carslaw and Jaeger 1947; Ingersoll, Zobal, and Ingersoll 1954). Given the rate of heat input to the loop and the inlet and outlet temperatures as a function of time, the effective thermal conductivity of the soil formation can be determined. A problem with this method, however, is that it assumes the rate of heat input to the water loop to be constant. This is rarely the case, since in the field the heater is usually powered by a portable generator. Even where line electrical service is available, short-term sags and swells in voltage may cause variations in heat input to the water loop. The random variation in power input — as well as random errors in the temperature measurements — presumably cause variations in the value of thermal conductivity obtained from a particular experiment, but the classical theory provides no information on the variance. Another area of uncertainty is when to begin measuring inlet and outlet temperatures and for how long the data should be collected — i.e., the period during which the line source model is valid.

In the cylinder source method, ground heat exchangers are modeled as a cylindrical, constant heat source in an infinite medium (Ingersoll, Zobal, and Ingersoll 1954). Deerman and Kavanaugh (1991) extended this model to account for variable heat flux, but in a manner not generally suitable for the analysis of short-term field data. Other authors (Eskilson 1987; Hellstrom 1991; Rottmayer, Beckmann, and Mitchell 1997; Austin 1998) have proposed more detailed two- and three-dimensional numerical models.

The method we describe in this report is based on a simple one-dimensional thermal model that describes the temperature field around the borehole. The inlet and outlet pipe flows are modeled as one, and a thin film may be added to account for the heat capacity of the pipes and the fluid. With this method, ground conductivity can be relatively accurately estimated even though the conditions at the borehole are uncertain.

Based on numerical solutions to the heat conduction equation in cylindrical coordinates, the parameter estimation method includes the effect of grout inside the borehole, allowing borehole resistance to be estimated in addition to soil thermal conductivity. This is significant because after soil thermal conductivity, borehole resistance is the most important parameter in the design of a vertical BHEx. In the absence of a method to measure borehole resistance, this parameter is usually calculated on the basis of the assumed thermal properties of the grout and U-tube piping, and the assumed spacing between the U-tube pipes (which some authors refer to as the shank spacing). Since the shank spacing is never accurately known once the U-tube goes into the ground, and the thermal properties of the grout are rarely measured on-site, a borehole resistance calculated in this manner may be very different from the actual value. Measuring borehole resistance at the site will reduce this uncertainty.

Another benefit to the method we have developed is that because the heat conduction problem is solved numerically rather than analytically, it is not necessary to assume constant heat input to the water loop. The heat transfer model uses the field-measured power input data rather than an average value. This feature is particularly useful in situations where unstable voltage (either from the power line or from the output of a portable generator) causes the power input to the water loop to vary over time. Because the line source and cylinder source methods both assume constant power input, their estimates of soil thermal properties tend to be inaccurate when the power input varies significantly.

A further benefit to our method is that it provides statistical estimates of the confidence intervals for the parameters estimated. Other methods of determining effective thermal properties have traditionally reported only the parameter value itself, with no estimate of accuracy. Obviously, the accuracy of a particular parameter value determined from a field experiment depends upon the accuracy of the data collection equipment, the length of the experiment, and other factors. The model we propose uses a statistical technique to provide a quantitative estimate of the confidence interval for the parameters measured.

The remainder of this section describes the theory behind our method.

2.2 THE PHYSICAL PROBLEM

Because the ground is not homogeneous in composition or density, and is affected by the presence of moisture, ground thermal properties can vary significantly with depth. A cross-section of a borehole of radius r_0 is shown in Fig. 2.1. The inlet and outlet pipes have an inside radius of a and are surrounded by grout to a radius r_0. The temperatures of the fluid in the inlet and outlet pipes are considered to be only a function of axial position, x. The temperature of the fluid in the pipes does change with time, but the time constant of the fluid is assumed to be much smaller than that for the heat conduction in the ground. Hence, the fluid heat transfer in the pipes is modeled in a steady-state manner; however, the heat capacity of the fluid is lumped into a "film" because the turbulent flow causes negligible radial temperature variation in the fluid. The temperature variations of the fluid in the axial direction are averaged so that the inlet and outlet temperatures appear.

The energy transferred from the borehole (or to the borehole) is absorbed by the surrounding ground, with most of the energy absorbed some distance away from the borehole. As the cooling (or heating) time increases, the thermally affected region becomes larger — that is, the temperature penetration increases with time. Moreover, as the distance from the borehole increases, the temperature distribution becomes one-dimensional. Since the thermally active region increases with time and becomes one-dimensional away from the centerline of the borehole, the temperature distribution at a large distance from the U-tube is similar to that which would be caused by a single pipe with an effective radius.

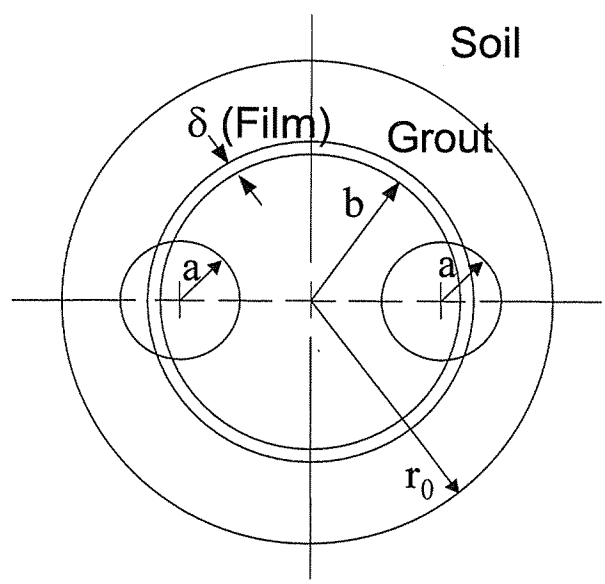

Fig. 2.1. Geometry of the borehole heat exchanger.

The two pipes in the borehole are encased in a grout whose thermal properties are generally different from

the thermal properties of the surrounding ground. The spacing (also called the shank distance) of the two pipes is difficult to maintain in the x direction, and the distances of the pipes from the edge of the borehole vary. The presence of the grout and the geometrical arrangement of the pipes is modeled by a single pipe of radius b. A thin film of thickness δ at the radius b is included to incorporate the heat capacity of the fluid in the pipes and any differential heat capacity in the grout compared to that in the surrounding ground. The film's heat capacity is an additional parameters that can be estimated along with the ground thermal conductivity.

Without loss of generality but for simplicity in thinking, the inlet pipe is assumed to have hot fluid entering it at a mass flow rate of $m = \rho VA$, kg/s, where ρ is density, V is fluid velocity and A is the cross-sectional area of a pipe, πa^2. See Figs. 2.1 and 2.2. The heat flux $q_h(x,t)$, W/m^2, is leaving the hot fluid and entering the surroundings. The other pipe is assumed to have the same fluid flow rate leaving and to be heated with a heat flux $q_c(x,t)$.

In the following sections we will first consider the fluid model based on an overall thermal control volume, and then the heat conduction in the ground.

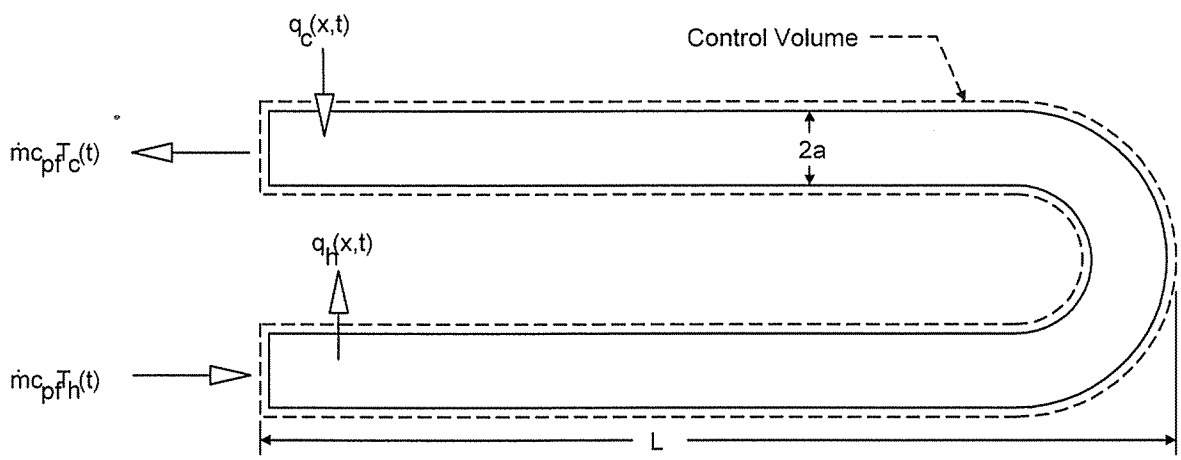

Fig. 2.2. Control volume for thermal analysis of borehole heat exchanger.

2.3 ENERGY FLUID MODEL

An energy balance on the fluid for the total length and for both pipes (see Fig. 2.2) gives

$$mc_{pf}\left[T_h(0,t) - T_c(0,t)\right] = \int_{x=0}^{L}\left[q_h(x,t) - q_c(x,t)\right]P\,dx = 0 \quad . \tag{2.1}$$

The inflow hot fluid temperature, $T_h(x,t)$, and the outflow cold fluid temperature, $T_c(x,t)$, are functions of time, but the rate of energy stored in the fluid is not included in Eq. (2.1). Energy absorbed by the fluid is lumped into an effective heat capacity of a thin film at the effective radius, b. The symbol P denotes the effective pipe perimeter; $q_h(x,t)$ and $q_c(x,t)$ are the hot and cold side heat flux, respectively, and c_{pf} is the specific heat of the fluid.

Because Eq. (2.1) does not account for the heat stored by the fluid and the pipes, it is accurate only for steady-state conditions; however, since the time constant for the fluid is assumed to be much

shorter than that of the surrounding soil, modeling the fluid heat transfer as a steady-state process should not introduce large errors. As shown below, the heat stored by the fluid and piping will be included in another manner.

In the grout and the soil, heat transfer takes place through conduction. The energy transferred from the U-tube is absorbed by the grout and eventually by the surrounding soil. As the heating (or cooling) time increases, the thermally affected region becomes larger—that is, the thermal penetration increases with time. Moreover, as the distance from the borehole increases, the temperature distribution becomes one-dimensional in the r-direction. This suggests that the temperature distribution in the soil at a large distance from the U-tube is similar to that which would be caused by a single pipe with some effective radius. Thus, in the model developed below, the two pipes of the U-tube are replaced by a single pipe with an effective radius, as shown in Fig. 2.1

2.4 ENERGY MODEL FOR SOIL, GROUT, AND FILM

The one-dimensional model for heat transfer in the soil is the transient heat conduction equation. One equation is required for the thermal resistive film, another for the grout, and another for the surrounding soil. The model for the soil is

$$\frac{k_s}{r}\frac{\partial}{\partial r}\left(r\frac{\partial T_s}{\partial r}\right) = (\rho c)_s \frac{\partial T_s}{\partial t}, r_0 < r < \infty \tag{2.2}$$

where the subscript s denotes soil.

The grout is considered to extend from $b+\delta$ to r_0. The energy equation for the grout is similar to Eq. (2.2) with s replaced by g for grout,

$$\frac{k_g}{r}\frac{\partial}{\partial r}\left(r\frac{\partial T_g}{\partial r}\right) = (\rho c)_g \frac{\partial T_g}{\partial t}, b+\delta < r < r_0 \quad . \tag{2.3}$$

Finally, a similar equation is written for the film, which extends from b to $b+\delta$:

$$\frac{k_t}{r}\frac{\partial}{\partial r}\left(r\frac{\partial T_t}{\partial r}\right) = (\rho c)_t \frac{\partial T_t}{\partial t}, b < r < b+\delta \quad , \tag{2.4}$$

where the subscript t denotes the thin film. The radius b is the effective radius, which is used to lump both pipes into one in the analysis. In Eqs. (2.2), (2.3), and (2.4) the temperature is a function of r, x, and t but the heat conduction in the x direction is assumed to be negligible compared to that in the r direction. Hence, the net heat conduction term in the x direction, $k\,\partial^2 T/\partial x^2$, is not included in these equations.

The boundary condition at the effective pipe radius (where the film of thickness, δ, is located) is

$$-k_t \frac{\partial T_t(b,x,t)}{\partial r} = q_h(x,t) - q_c(x,t) \quad , \tag{2.5}$$

which applies at each x; however, it is more convenient to average over x in Eq. (2.5) and also in Eqs. (2.2), (2.3), and (2.4). Integrating Eq. (2.5) from $x = 0$ to L gives

$$-k_f \frac{\partial \overline{T}_f(b,t)}{\partial r} = \frac{1}{L} \int_{x=0}^{L} \left(q_h(x,t) - q_c(x,t)\right) dx \quad , \tag{2.6}$$

where

$$\overline{T}_f(b,t) = \frac{1}{L} \int_{x=0}^{L} T_f(b,x,t) dx \quad . \tag{2.7}$$

The differential equations for the conduction in the soil, grout, and film are now averaged over x from 0 to L. Equations (2.2), (2.3), and (2.4) become

$$\frac{k_s}{r} \frac{\partial}{\partial r}\left(r \frac{\partial \overline{T}_s}{\partial r} \right) = (\rho c)_s \frac{\partial \overline{T}_s}{\partial t}, r_0 < r < \infty \tag{2.8}$$

$$\frac{k_g}{r} \frac{\partial}{\partial r}\left(r \frac{\partial \overline{T}_g}{\partial r} \right) = (\rho c)_g \frac{\partial \overline{T}_g}{\partial t}, b + \delta < r < r_0 \tag{2.9}$$

$$\frac{k_f}{r} \frac{\partial}{\partial r}\left(r \frac{\partial \overline{T}_f}{\partial r} \right) = (\rho c)_f \frac{\partial \overline{T}_f}{\partial t}, b < r < b + \delta \tag{2.10}$$

where the average temperatures are defined by

$$\overline{T}_s(r,t) = \frac{1}{L} \int_{x=0}^{L} T_s(r,x,t) dx \quad , \tag{2.11}$$

$$\overline{T}_g(r,t) = \frac{1}{L} \int_{x=0}^{L} T_g(r,x,t) dx \quad , \tag{2.12}$$

$$\overline{T}_f(r,t) = \frac{1}{L} \int_{x=0}^{L} T_f(r,x,t) dx \quad . \tag{2.13}$$

A complete mathematical statement is then Eqs. (2.8), (2.9), and (2.10) with the boundary condition at $r = b$ given by Eq. (2.6) and the interface conditions given by

$$k_f \frac{\partial \overline{T}_f(b+\delta,t)}{\partial r} = k_g \frac{\partial \overline{T}_g(b+\delta,t)}{\partial r} \quad , \tag{2.14}$$

$$\overline{T}_f(b+\delta,t) = \overline{T}_g(b+\delta,t) \quad , \tag{2.15}$$

$$k_g \frac{\partial \overline{T}_g(r_0,t)}{\partial r} = k_s \frac{\partial \overline{T}_s(r_0,t)}{\partial r} \quad , \tag{2.16}$$

$$\overline{T}_g(r_0,t)=\overline{T}_s(r_0,t) \quad . \tag{2.17}$$

The boundary condition given by Eq. (2.6) can also be related to the input and output fluid temperatures to get the alternate boundary condition,

$$-k_f\frac{\partial\overline{T}_f(b,t)}{\partial r}=\frac{mc_{pf}}{PL}\left[T_h(0,t)-T_c(0,t)\right] \quad . \tag{2.18}$$

The boundary condition at $r = \infty$ is

$$\overline{T}_s(\infty,t)=T_\infty \quad , \tag{2.19}$$

and the initial conditions are

$$\overline{T}_s(r,0)=T_\infty,\overline{T}_f(r,0)=T_\infty,\overline{T}_g(r,t)=T_\infty \quad . \tag{2.20}$$

The ratio mc_{pf}/PL in Eq. (2.13) is also equal to

$$\frac{mc_{pf}}{PL}=\frac{G\pi a^2c_{pf}}{2\pi bL}=\frac{Ga^2c_{pf}}{2bL} \quad , \tag{2.21}$$

where G is the mass flux in kg/m^2-s.

The boundary condition given by Eq. (2.18) can also be written as

$$-k_f\frac{\partial\overline{T}_f(b,t)}{\partial r}=q_0(t) \quad , \tag{2.22}$$

where the heat flux $q_0(t)$ is the field-measured heat flux divided by the borehole depth L.

In summary, the direct problem is described by Eqs. (2.8), (2.9), and (2.10) with interface conditions, Eqs. (2.14) through (2.17); the condition at infinity, Eq. (2.19); and initial conditions, Eq. (2.20). The boundary condition at $r = b$ is Eq. (2.22).

The equations above are a complete mathematical statement of the direct problem. However, the problem cannot be solved with classical techniques because not all of the relevant parameters (such as the ground and film thermal conductivities) are known. Some extra information is available that allow these and other parameters to be estimated. The average fluid temperature, defined by the average of the inlet and outlet temperatures, is known:

$$Y_f=\left(T_h(t)+T_c(t)\right)/2 \quad . \tag{2.23}$$

This average temperature may not be precisely equal to the integrated averages of the inlet and outlet fluid temperatures but is expected to be as accurate as the lumping of the two pipes into one. Furthermore, the inlet and outlet temperatures are the only temperatures that are measured. This temperature is equal to the average of the surface film temperature given by Eq. (2.6). Hence, two conditions are given at the film surface: heat flux and temperature histories. For direct problems only

one condition can be used; thus, there is excess information. This information is used to estimate one or more parameters in a least squares sense. The Y symbol is used in Eq. (2.19) to denote a measured quantity.

The calculated average surface temperature history given by Eq. (2.6) is made to agree in a least squares sense with the measured average fluid temperature given by Eq. (2.19) by minimizing a sum of squares function with respect to parameters, such as the ground thermal conductivity. The sum of square function, S, is

$$S = \sum_{i=1}^{n} \left(Y_i - T_{t,i} \right)^2 \quad , \tag{2.24}$$

where i denotes a measurement time, Y_i the average fluid temperature, and $T_{t,i}$ the average temperature of the film at $r = b$.

Note that if the film thickness is taken to be zero, if the film is assumed to have no volumetric heat capacity and no resistance to heat transfer, and if the grout has the same thermal properties as the soil, then the problem reduces to that of a cylindrical heat source in an infinite medium. For constant heat flux, this problem has an analytical solution involving a rather complicated integral of Bessel and other functions (Ingersoll, Zobal, and Ingersoll, 1954). The method can be extended to the case of non-constant heat flux using a convolution process, but this is difficult to implement numerically. For this reason, and so that the effect of the thin film and the grout can be included, we solve the direct problem numerically using a finite difference grid and a Crank-Nicolson integration scheme.

Altogether, the model presented above contains nine parameters: the thermal conductivities of the soil, grout, and thermal film; the volumetric heat capacities of the soil, grout, and thermal film,; the thickness of the thermal film; the effective pipe radius, and the far-field temperature. In general, however, it will not be possible to estimate all of these parameters with a single experiment, as some may be dependent on others. For example, since the thin film is used to account for the thermal capacitance of the fluid and pipes, we would expect the thickness, δ, to be related to the film's volumetric heat capacity.

The parameter estimation algorithm proceeds by first assuming trial values for the parameters in question. Given these values, the (measured) heat flux is used to drive the numerical model. The numerical model gives a predicted value of T_t as a function of time for the duration of the experiment. The sum of squared errors between the predicted and measured temperatures are calculated as in Eq. (2.20). The Gauss method of minimization is then used to determine the parameter values that minimize the sum of the squared errors.

While the derivation is beyond the scope of this report, use of the Gauss minimization technique enables calculation of approximate confidence regions for the parameters (Beck and Arnold 1977). The validity of these confidence intervals depends on a number of statistical assumptions that may or may not be satisfied in a given experiment. A number of other sources of error are unaccounted for by these confidence intervals: the assumption that the soil properties are homogeneous, when in fact they vary with depth; the assumption that the far-field temperature, T_∞, is accurately measured; and of course, the assumption that a rather complicated three-dimensional heat transfer process can be represented by a one-dimensional model. For this reason we expect the confidence intervals derived from the data to be somewhat smaller than the true confidence intervals; the true confidence intervals on the parameter estimates may be as much as twice the value indicated. Nevertheless, these

approximate confidence intervals are useful for qualitative assessment of the accuracy of property values and for comparing one experiment to another.

2.5 THE GPM SOFTWARE

The method described above has been incorporated into a stand-alone software program called GPM (geothermal properties measurement). The program requires as input a text file containing average fluid temperature (i.e., the average between U-tube inlet and outlet temperatures) and heat input at constant time intervals. This data is usually measured in a short-term in situ field test. The program uses parameter estimation techniques to determine the soil formation thermal properties that best match the data.

As indicated in Section 2.4, the model described above includes no fewer than nine parameters that could potentially be determined by way of parameter estimation: the thermal conductivities of the soil, grout, and thermal film; the volumetric heat capacities of the soil, grout, and thermal film; the thickness of the thermal film; the effective pipe radius; and the far-field temperature. In general, however, it is not possible to estimate all of these parameters with a single experiment. The GPM program provides the option to determine (*a*) soil thermal conductivity and far-field temperature or (*b*) soil thermal conductivity, borehole resistance, and far-field temperature. Chapter 3 presents the results of a validation study of the GPM software, and Chapter 4 provides a brief user's manual.

2.6 CONCLUSIONS

The one-dimensional parameter estimation model describes the thermal behavior of a borehole heat exchanger for a GHP. The model lumps the inlet and outlet pipes into one pipe of an effective radius b and adds a film at the outer surface of the pipe to account for the heat transfer resistance of the surrounding grout and the convective heat transfer coefficient. The film also has an effective heat capacity to model the heat capacity of the fluid and the different heat capacity of the grout compared to the ground. Parameter estimation techniques are used to derive values of soil and grout thermal conductivity from the model and experimental data. An important feature of this technique is that it provides approximate confidence intervals on the parameter estimates; these intervals can be used to assess the accuracy of experiments and the thermal conductivities derived from such experiments.

3. FIELD TESTS OF THE GPM SOFTWARE

3.1 FIELD RIG TESTS

A major problem in validating a model such as the one presented in Chapter 2 is that the true soil formation thermal properties at a given site are generally unknown. Where estimates of these properties are available, they are usually based on previous experiments and other simplified heat transfer models such as the line heat source. Recently, however, a test rig was constructed at Oklahoma State University to simulate the conditions in which a vertical heat exchanger operates. The rig consists of a box made of ¾-in. plywood, with approximate dimensions of 4 × 4 × 48 ft. A U-tube heat exchanger consisting of nominal 1-in.-diam polyethylene piping is placed horizontally along the centerline of the box, parallel to the long axis. The U-tube is grouted to a diameter of 5 in. from the centerline, and the box is filled with a homogeneous material with known thermal conductivity. As in a field experiment, water is heated and pumped through the U-tube at a known flow rate while the rate of heat input and inlet and outlet water temperatures are measured at regular intervals. Although we recognize that this rig does not exactly duplicate the heat transfer processes that take place in a vertical heat exchanger in a field installation, it does provide an opportunity to build confidence in heat transfer models such as the one we have developed, since the material which represents the soil is homogeneous, and its thermal conductivity can be measured independently.

A data set from a 63-h experiment was obtained from Dr. Marvin Smith (personal communication from M. Smith, Oklahoma State University, to J. Shonder, March 1998). For the experiment the rig was filled with wet sand, and the U-tube was grouted with a commercially available grout. The thermal conductivity of the sand was measured twice using a thermal probe, giving values of 1.40 and 1.45 Btu/hr-ft-°F. At the beginning of the experiment the sand was at a uniform temperature of 72.0°F. During the experiment, the average flow rate of water was approximately 4 gal/min, and the average rate of heat input was 363 W. Both of these values varied by only about ±0.5% of their average values over the 63-h period. Water inlet and outlet temperature, flow rate, and power to the heater were measured at 1-min intervals.

To analyze the experimental data, some modifications were made to the model to account for the physical characteristics of the test rig. Since the model is radially symmetrical, the rig was modeled as a cylinder consisting of four regions with different materials. The U-tube was modeled as a single pipe with an effective diameter of 0.75 in. (A value of 0.5 in. was also used; as discussed below, the effective pipe diameter appears to have only a small effect on the thermal property estimates.) A thin film is assumed to exist at the surface of the pipe to simulate the heat capacity of the water and the pipes; the film is assumed to be 0.024 in. thick. The diameter of the grout is given as 5 in.; thus, the material from the outer edge of the thin film to a radius of 2.5 in. is assumed to be grout. The bulk of the region is the sand, from the outer radius of the grout to an effective radius of 2.246 ft. Plywood with a thickness of 0.75 in. is at the outer radius. To summarize, in the radial direction there is the film, grout, sand, and plywood. The finite difference model includes 72 nodes: 2 in the film, 6 in the grout, 60 in the sand, and 4 in the plywood. The internal time step was 15 s. In the analysis, the outer boundary of the plywood is assumed to be isothermal at the initial temperature of 72.0°F. A volumetric heat capacity of 35 Btu/ft^3-hr was assumed for both the sand and the grout. The thermal conductivity of the film was assumed to be a large value; thus, all of the resistance to heat transfer is contained in the soil and the grout. Three parameters are estimated: the thermal conductivity of the soil, the thermal conductivity of the grout, and the volumetric heat capacity of the thin film.

Fig. 3.1 plots the measured average water temperature and the model's predicted average temperature for the first 30 h of the experiment, at the converged values of the parameters. There is excellent agreement between the two. In order to distinguish between model and data, the predicted water temperature is plotted only at intervals of 1 h. Figure 3.2 presents the residuals — i.e., the difference between the measured and predicted average water temperature — as a function of time for the first 30 h. The larger residuals at early times are probably due to the assumption of one-dimensional heat transfer. However, since the largest residual is only 0.2°F, the error is not large. Although the residuals are small overall, with a root mean square (rms) value of 0.057°F, if the model were truly an accurate representation of the heat transfer process taking place in the test rig, we would expect the residuals to be random and uncorrelated, which they clearly are not. Their slow rise and fall over the 30 h indicates that there may be some secondary effects which the model does not capture.

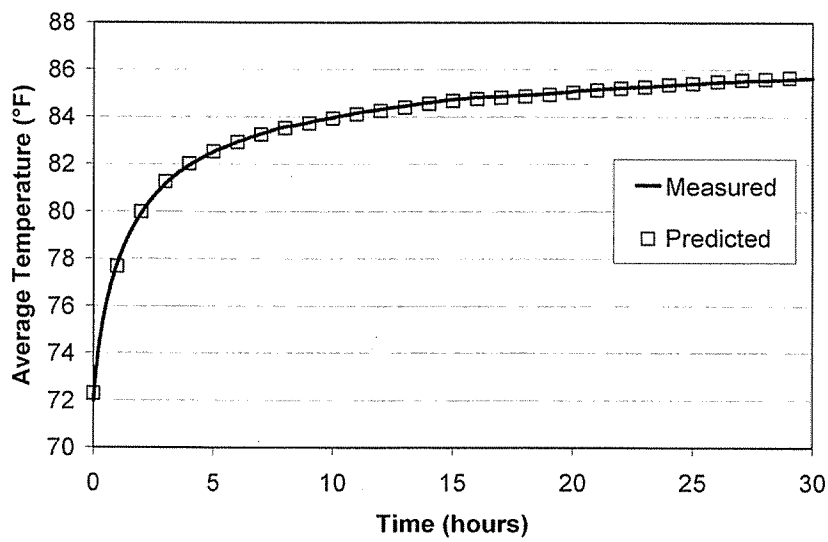

Fig. 3.1. Measured and predicted average water temperature for experiment using the Oklahoma State University test rig.

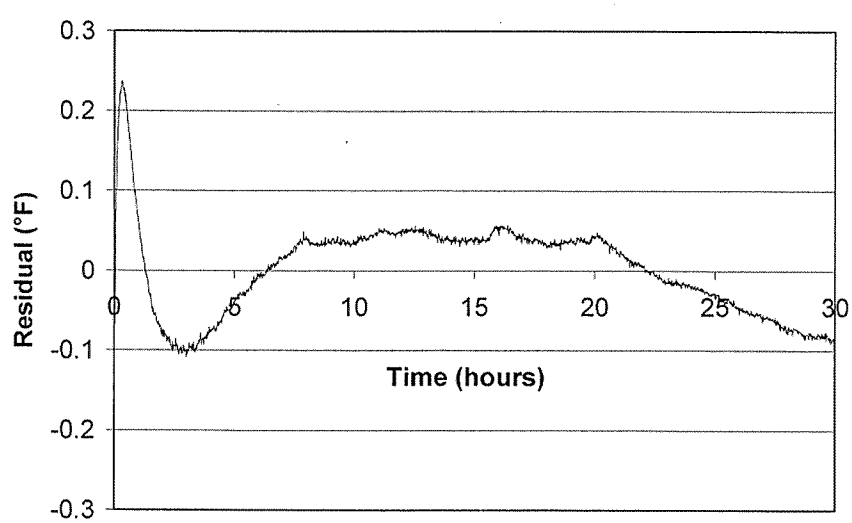

Fig. 3.2. Residuals for the experiment on the Oklahoma State University test rig.

The estimate of thermal conductivity from the model is in excellent agreement with the measured values. After 30 h the converged value of thermal conductivity for the wet sand is 1.411 Btu/hr-ft-°F, compared with the measured values of 1.40 and 1.45. The 95% confidence region for the thermal conductivity value is ±0.172 Btu/hr-ft-°F, or about 12% of the estimated value.

The converged value for the thermal conductivity of the grout is 0.619 Btu/hr-ft-°F with a 95% confidence region of 0.037 Btu/hr-ft-°F, which is about 6% of the estimated value. The actual thermal conductivity of the grout was not available, but the value of 0.619 Btu/hr-ft-°F is in the range of values reported in the literature. In any case, we expect that the estimated grout thermal conductivity accounts for other effects, such as the contact resistance between the pipes and the grout.

The time required to converge to a solution depends, of course, on the initial guesses for the parameter values. Nevertheless, even for guesses 50% larger than the true values, the model requires only about 60 s to converge on a 200-MHz PC.

We performed a second run assuming an effective pipe diameter of 0.5 in. In this case the converged value of the sand thermal conductivity was 1.421 ± 0.133 Btu/hr-ft-°F, which indicates that the effective pipe diameter has only a small effect on the thermal conductivity measurement. Bose, Parker, and McQuiston (1985) have recommended using an effective diameter of $\sqrt{2}$ times the diameter of the U-tube piping, which in this case would correspond to a radius of 0.707. Since there was little difference between the thermal conductivity estimates using effective radii of 0.5 and 0.75 in., we would agree with the recommendation of these authors.

The thermal property estimates changed somewhat when data up to 60 h were used. With an effective pipe radius of 0.75 in., the rms value of the residuals increased slightly, to 0.064°F. The converged value for the thermal conductivity for the sand increased to 1.558 ± 0.118 Btu/hr-ft-°F. This is higher than the value obtained after 30 h, but the measured value of thermal conductivity still lies within the 95% confidence region. The converged value of the grout thermal conductivity was slightly lower in this case, 0.593± 0.023 Btu/hr-ft-°F.

Sequential estimates of the sand and grout thermal conductivity are presented in Fig. 3.3. This figure shows, for each time, the values of the thermal conductivities estimated using all data up to and including that time. If the model were an accurate representation of the heat transfer processes taking place in the test rig, we would expect both curves to flatten out at later times. In the case of the grout thermal conductivity this does seem to occur; the estimate of the sand thermal conductivity appears to be rising slightly even at 60 h. This may be due to the assumptions made in the analysis, primarily the assumption that the rectangular test rig could be modeled as a cylinder. We would expect errors associated with this assumption to become more important at later times. Of course, this would not be a concern in a field test.

3.2. IN SITU TESTS AT TWO ELEMENTARY SCHOOLS

The tests at Oklahoma State University showed that our method could predict the thermal conductivity of a known material (moist sand) accurately, given data collected in an experiment on a laboratory test rig. However, further work was needed to validate the model and gain experience in its use. We also wanted to estimate other parameters, especially borehole resistance (the total resistance of heat transfer from the fluid to the borehole wall), a parameter that is required by many design algorithms. Therefore, we set up a series of field experiments in which the model's thermal conductivity estimates would be compared with estimates from other commonly used models and

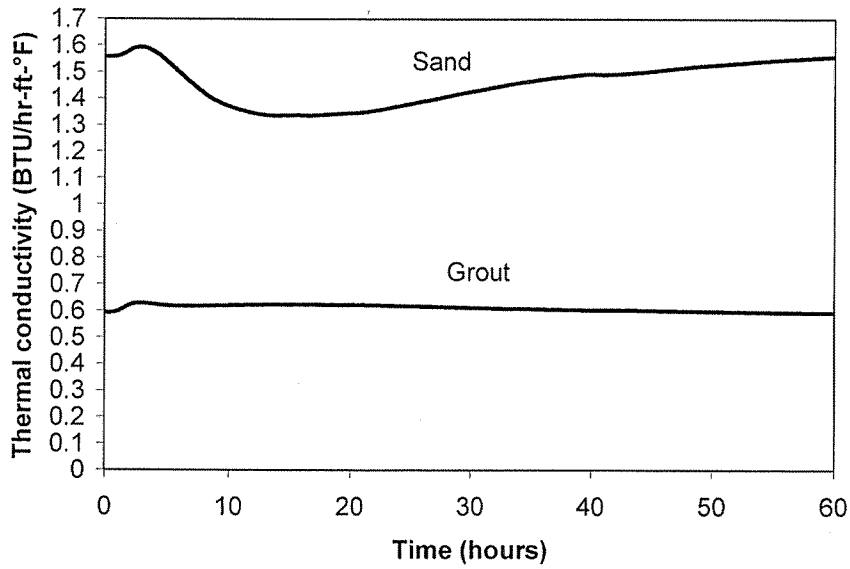

Fig. 3.3. Sequential estimates of sand and grout thermal conductivity.

with the "true" or effective thermal conductivity of the soil, determined from data on active borefields at the sites.

We conducted three in situ tests at two elementary schools, Maxey and Campbell, in Lincoln, Nebraska, in 1998 and 1999. Data from in situ field tests provide a more rigorous test of a properties measurement technique than data from laboratory experiments, but a field test has the drawback that the true thermal conductivity of the soil formation and borehole resistance at the site are generally unknown. For the Maxey School site, however, analysis of one year of data from the operating borefield provided an estimate for the effective soil thermal conductivity that could be compared with the measured values.

At Campbell Elementary School, two boreholes were drilled with the same diameter and the same approximate depth, about 60 ft apart. A third borehole was drilled at Maxey. Three different grouts were used: thermal grout 85, fine sand, and soil cuttings. The tests were blind in that the driller did not inform us of which grout was used in which borehole.

One objective of the in situ field tests was to determine whether the soil conductivity estimates for the two boreholes at Campbell agreed with each other and whether the conductivity estimate at Maxey agreed with the thermal conductivity estimate obtained from analysis of the operating data. Another objective was to determine whether the numerical method could identify the different borehole resistances resulting from the different grouts. Table 3.1 shows the parameters of the tests. For purposes of comparison, the three data sets were also analyzed using the line source and cylinder source methods.

3.2.1 Description of Tests

For each test, a 4.25-in. diameter borehole was drilled to an approximate depth of 245 ft. Nominal 1-in. SDR-11 U-tube pipe was inserted, and the boreholes were grouted with either thermal grout or

Table 3.1. Parameters of three in situ thermal properties tests performed at Lincoln, Nebraska, elementary schools

Test designation	Date performed	Borehole depth (ft)	Average soil temperature (°F)	Average power input (W)
Maxey	09/19/98	245	55.7	2609
Campbell #1	09/15/98	245	53.8	2595
Campbell #2	10/08/98	244	55.6	2606

fine sand, or not grouted at all. In general, the boreholes were drilled about 75 ft from the active borefield. The two boreholes at Campbell school were approximately 60 ft apart.

The equipment used to perform the in situ tests has been described by Austin (1998). Housed in a trailer that is towed to the site, the apparatus includes two circulating pumps, a flowmeter, and three in-line water heaters, all powered by a portable electric generator. A watt transducer measures the power consumption of the heaters and circulating pumps, and the inlet and outlet temperatures are measured using two high-accuracy thermistors immersed in the flow. The water flow rate, total power input, and inlet and outlet temperature were logged at 15-min intervals.

Before the U-tube was connected to the test apparatus, a thermistor was inserted into one end of the U-tube and the water temperature was measured at 10-ft intervals. The average undisturbed soil temperature at each site was assumed to be the average of these measurements. The actual length of the installed heat exchanger was also determined from these measurements.

Figures 3.4 and 3.5 present the power input and average water temperature as a function of time for the two experiments at Campbell School, and Fig. 3.6 presents the data for the experiment at Maxey School. The three tests are unremarkable except for the test on the second well at Campbell. Just noticeable in Fig. 3.5 are two jumps in average temperature at 27.5 h and at 33.5 h. Beginning at

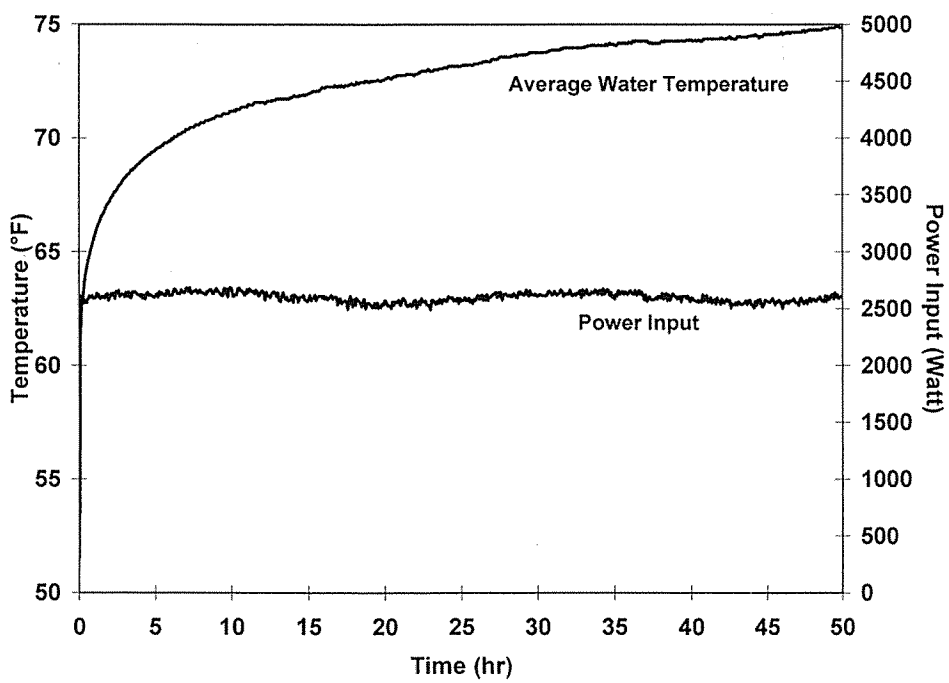

Fig. 3.4. Power input and average water temperature, Campbell Elementary School test #1.

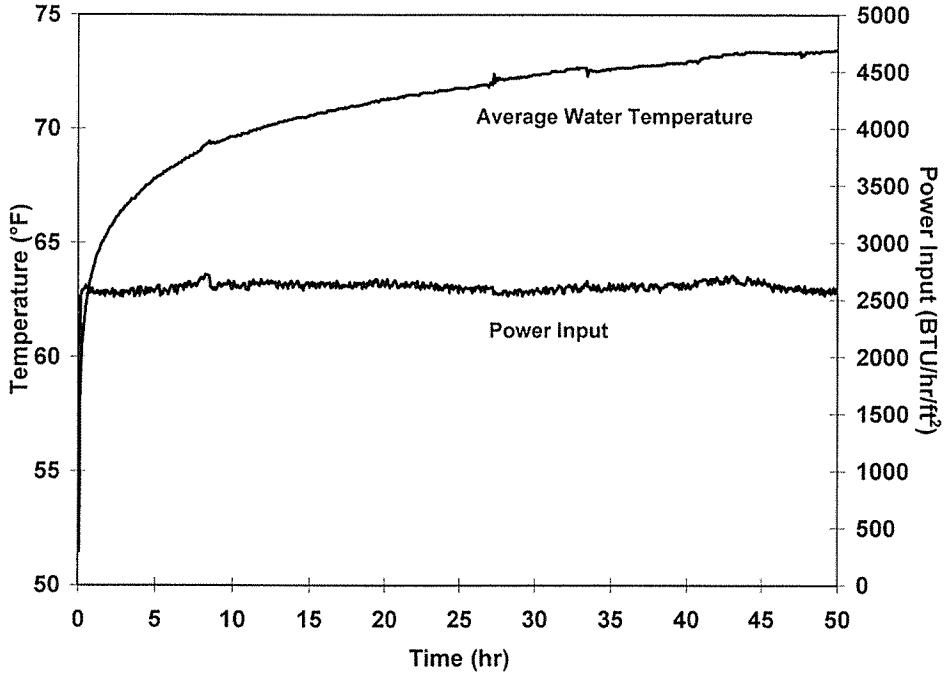

Fig. 3.5. Power input and average water temperature, Campbell Elementary School test #2.

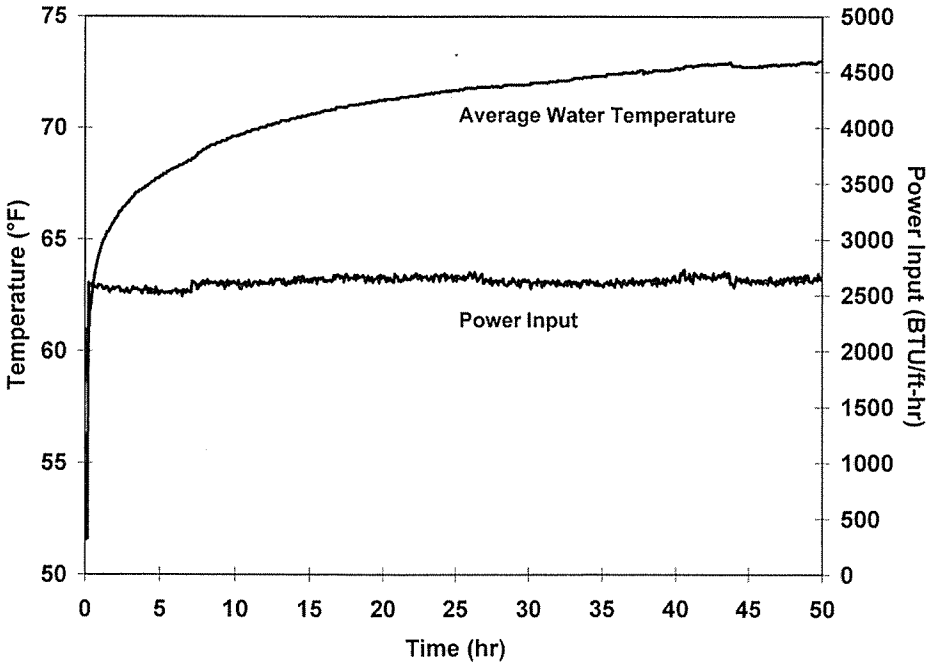

Fig. 3.6. Power input and average water temperature, Maxey Elementary School test #1.

27.5 h, the water flow rate through the heat exchanger dropped by about 15%, possibly due to the presence of air in the heat exchanger. This does not appear to have affected the accuracy of the parameter estimates.

3.2.2 Test Results

One indication of a model's reliability is its ability to predict the temperature rise of the water as a function of time. Although the one-dimensional numerical model includes a number of simplifications, it is able to predict the average water temperature in the heat exchanger with good accuracy. Figures 3.7 through 3.9 present plots of the residuals between the measured and predicted average temperature as a function of time. For times after about 30 min, the residuals are quite small, on the order of 0.17°F. The model did not accurately follow the system behavior during the sharp decrease in flow rate that occurred during the second Campbell experiment, but again, this did not seem to affect the property estimates in that case.

Thermal Conductivity

Table 3.2 presents the estimates for soil thermal conductivity and borehole resistance. There is good agreement between the two thermal conductivity measurements at each site. The value of 1.36 obtained for the Maxey test agrees well with the value of 1.3 obtained from analysis of a year's operating data from the borefield (Thornton 1999). The average of the two Campbell measurements is 1.20 BTU/hr-ft-°F, and the two tests were consistent with one another (the thermal conductivity estimates differ by only 2%), so it appears there is a definite difference between soil thermal conductivity at the two schools.

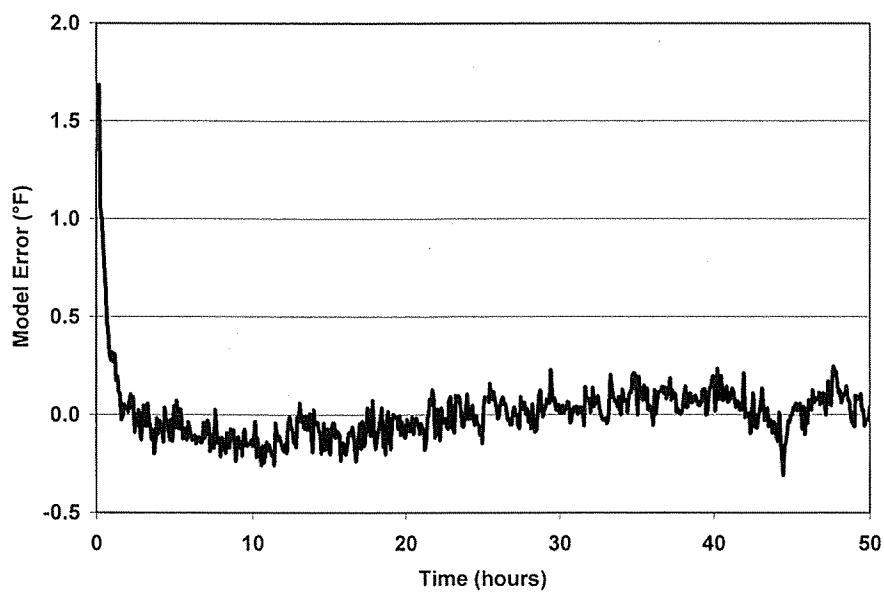

Fig. 3.7. Model error ($T_{measured} - T_{calculated}$) for Campbell Elementary School test #1.

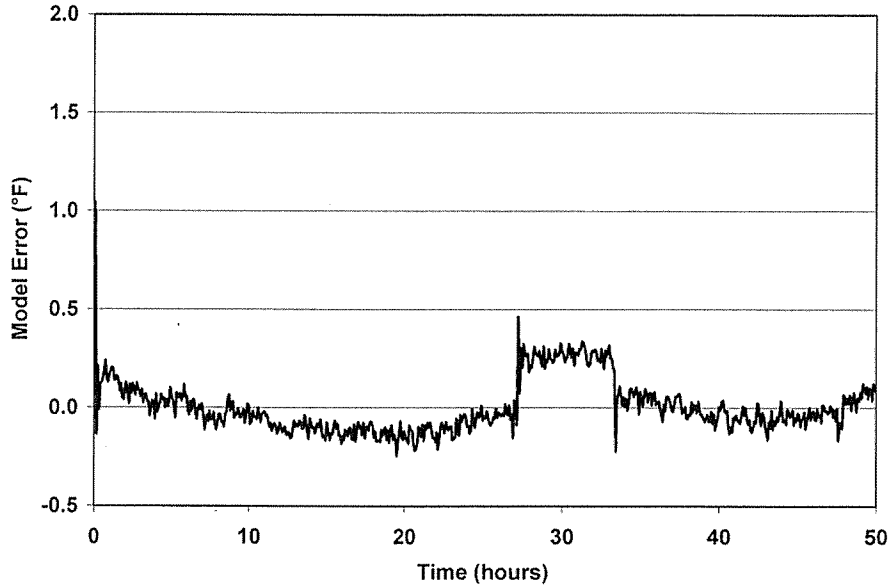

Fig. 3.8. Model error ($T_{measured} - T_{calculated}$) for Campbell Elementary School test #2.

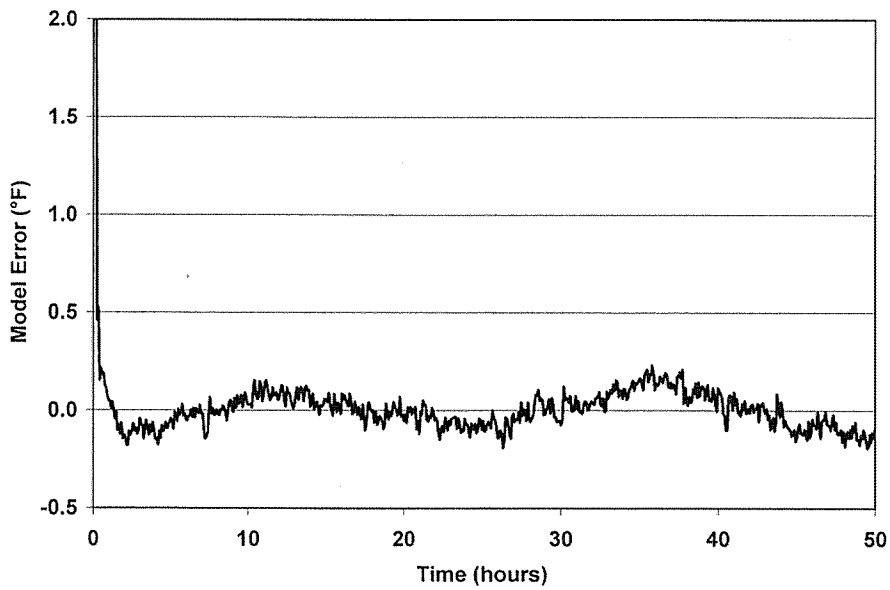

Fig. 3.9. Model error ($T_{measured} - T_{calculated}$) for Maxey Elementary School test #1.

Table 3.2. Results of soil thermal conductivity and borehole resistance estimates from three in situ tests

Test designation	Soil thermal conductivity (BTU/hr-ft-°F)	Borehole resistance (hr-ft-°F/BTU)	Grout material
Maxey	1.36±.02	0.185±.003	Thermal grout 85
Campbell #1	1.20±.04	0.226±.015	Soil cuttings
Campbell #2	1.19±.03	0.158±.008	Fine sand

Borehole Resistance

Although Table 3.2 indicates a definite difference between the borehole resistances measured at each site, it is difficult to say whether the measured borehole resistances correspond to the expected values. For a given U-tube size, borehole resistance is a function of grout thermal conductivity and shank spacing. Spitler (1996) has developed a spreadsheet program that is useful for calculating borehole resistance given shank spacing and grout conductivity. As an example, for a 1-in. SDR-11 U-tube grouted with thermal grout 85 (nominal thermal conductivity of 0.85 Btu/hr-ft-°F), the spreadsheet calculates borehole resistances between 0.176 and 0.313, depending on the shank spacing assumed. The measured borehole resistance for heat exchanger #1 at Maxey School does lie within this range, and the fact that it is closer to the lower limit may indicate that the U-tube legs are close to the borehole wall.

Determining the borehole resistance of the heat exchangers grouted with fine sand is more problematic, since the thermal conductivity of sand depends on moisture content. With a nominal value of 1.5 Btu/hr-ft-°F for the sand thermal conductivity, the calculated borehole resistance is between 0.139 and .237. The measured resistances for Maxey test #2 and Campbell test #2 are both within these limits, and both are closer to the lower limit than the higher one, indicating again that the U-tube legs may be close to the borehole wall.

Heat exchanger #1 at Campbell school was grouted with soil cuttings. If the grout is assumed to have the same thermal conductivity as the soil, the calculated borehole resistance would lie between 0.151 and 0.248. The measured borehole resistance does in fact lie between these limits, but certainly, further experiments would have to be conducted to determine whether borehole resistance can be measured reliably with this method.

3.2.3 Comparison with Other Analysis Techniques

Table 3.3 compares the thermal conductivity estimates from the three tests using our numerical method with the values obtained using the line source and cylinder source methods. These are 50-h estimates. For the line source method, data prior to 4 h was ignored. In general the parameter estimates agree well with the estimates using the line source and cylindrical source methods, with differences on the order of only 2 to 3%.

Table 3.3. Thermal conductivity estimates derived by three test methods from 50-h tests

Test designation	Numerical method	Line source method	Cylinder source method
Maxey	1.36	1.30	1.39
Campbell #1	1.20	1.24	1.19
Campbell #2	1.19	1.18	1.22

In addition to comparing the 50-h thermal conductivity estimates, it is also informative to examine plots of sequential estimates from the three methods. These plots show, for every time, the estimate of thermal conductivity obtained by using all the data up to that time. A plot of sequential parameter estimates can indicate whether the method is converging to a particular value, or whether the estimate changes significantly over time. Sequential plots are also useful for estimating how long the data must be collected in order to obtain an accurate parameter estimate.

Figures 3.10 through 3.12 present sequential thermal conductivity estimates for the three experiments from 10 to 50 h, using the one-dimensional numerical method, the line source method, and the cylinder source method. Data prior to the fourth hour was ignored for the line source analysis, and a volumetric heat capacity of 30 Btu/ft^3-°F was assumed for both the one-dimensional numerical method and the cylinder source method. For the two Campbell tests, all three methods converged to within about 5% of their 50-h values within 24 h (Figs. 3.10–3.11). This was not the case with the Maxey test, however (Fig. 3.12). Although the estimates from the three methods agree among each other, the plots in Fig. 3.12 suggest that had the measurements continued beyond 50 h, the thermal conductivity estimate at the Maxey site would have continued to rise. One possibility is that there is modest groundwater flow at the site. Conditions such as these, which vary from site to site, make it difficult to make general recommendations as to how long thermal conductivity tests should proceed.

The comparisons indicate that there is little difference between the thermal conductivity estimates derived from our method and the line source method. However, the stable power supply and otherwise good quality of the three data sets tend to mask the usefulness of the method we have developed. Figure 3.13 presents data from a thermal conductivity test carried out at another site. During this test, the field generator developed mechanical problems (personal communication from C. Remund, South Dakota State University, to J. Shonder, ORNL, April 1999). Our conversations with field personnel indicate that short-term voltage spikes are not uncommon, even when line power is used in place of a generator. These spikes can cause significant problems if the line source or cylinder source methods are used to estimate thermal conductivity because both methods assume that the power input is constant. The one-dimensional numerical method we have developed does not assume constant power. Because the model is driven with the field-measured power input, voltage spikes cause very little change in the thermal conductivity estimates.

Figure 3.14 is a plot of sequential thermal conductivity estimates from the data of Fig. 3.13 derived using the line source method, the cylinder source method, and our one-dimensional numerical method. Because the cylinder source method calculates thermal conductivity based only on the measured temperature rise for a particular time, it is much more sensitive to short-term variations in power. For example, between 30 and 33 h the cylinder source estimate of thermal conductivity drops by almost 10%, owing primarily to fluctuations in the power input. The line source method is somewhat less affected by short-term fluctuations because it uses all of the temperature data up to a given time. Nevertheless, the line source method still assumes constant power input, and this can cause abrupt changes in the thermal conductivity estimate. Our one-dimensional numerical method is the most stable of all because it uses all of the power data and all of the temperature data. As shown in Fig. 3.14, the estimate of thermal conductivity from our method changes by only 1 to 2% over the entire experiment.

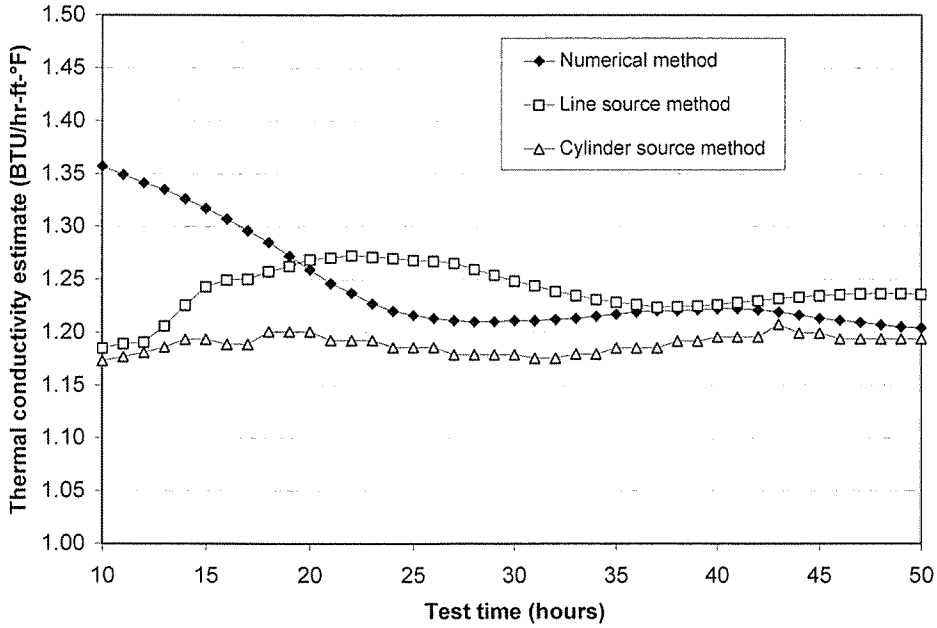

Fig. 3.10. Sequential thermal conductivity estimates, Campbell Elementary School test #1.

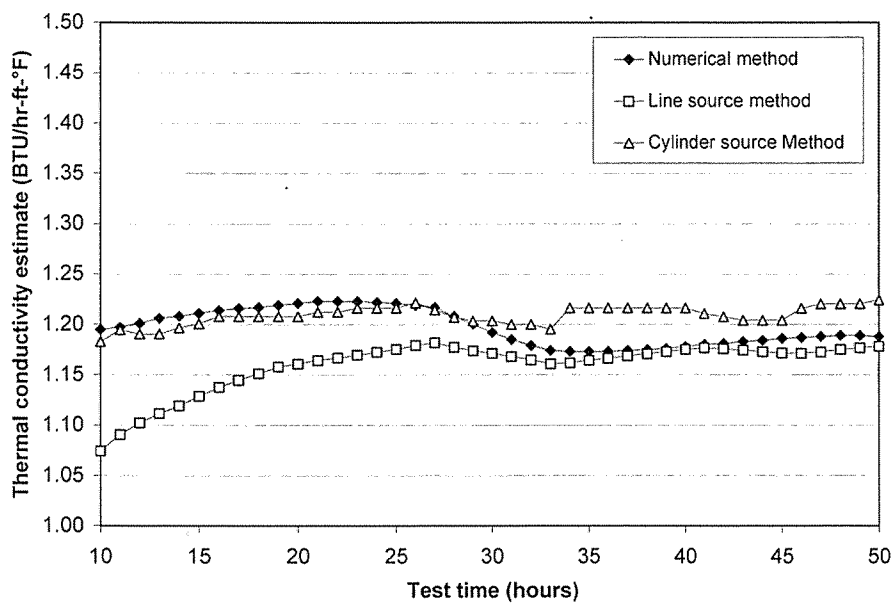

Fig. 3.11. Sequential thermal conductivity estimates, Campbell Elementary School test #2.

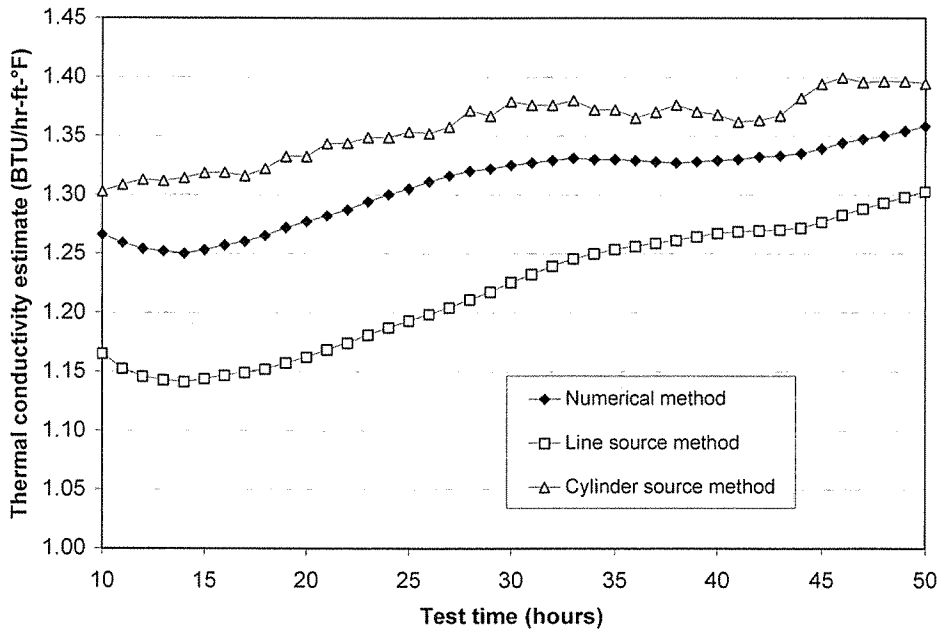

Fig. 3.12. Sequential thermal conductivity estimates, Maxey Elementary School test #1.

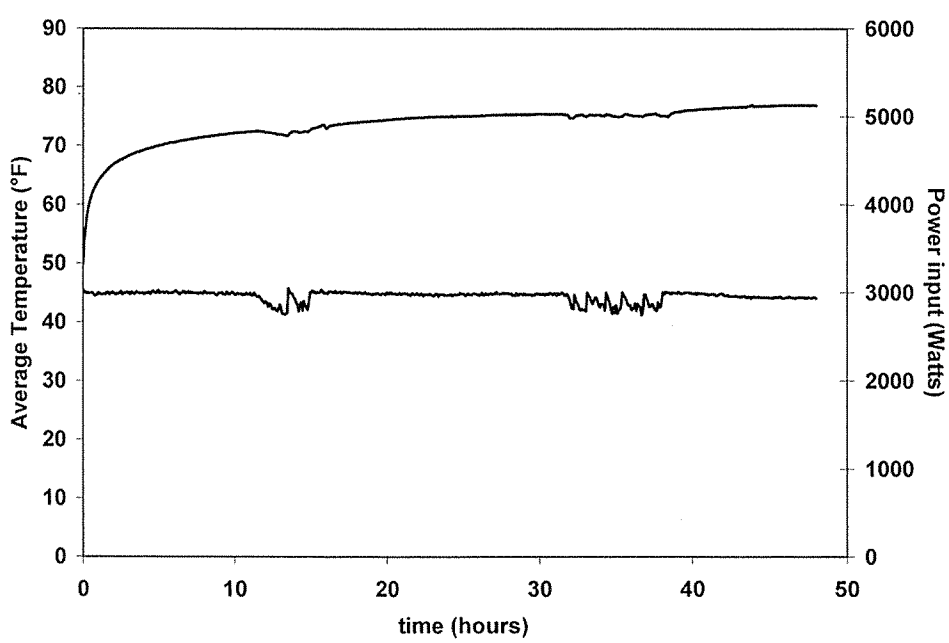

Fig. 3.13. Temperature and power input vs time for a case in which the generator developed mechanical problems.

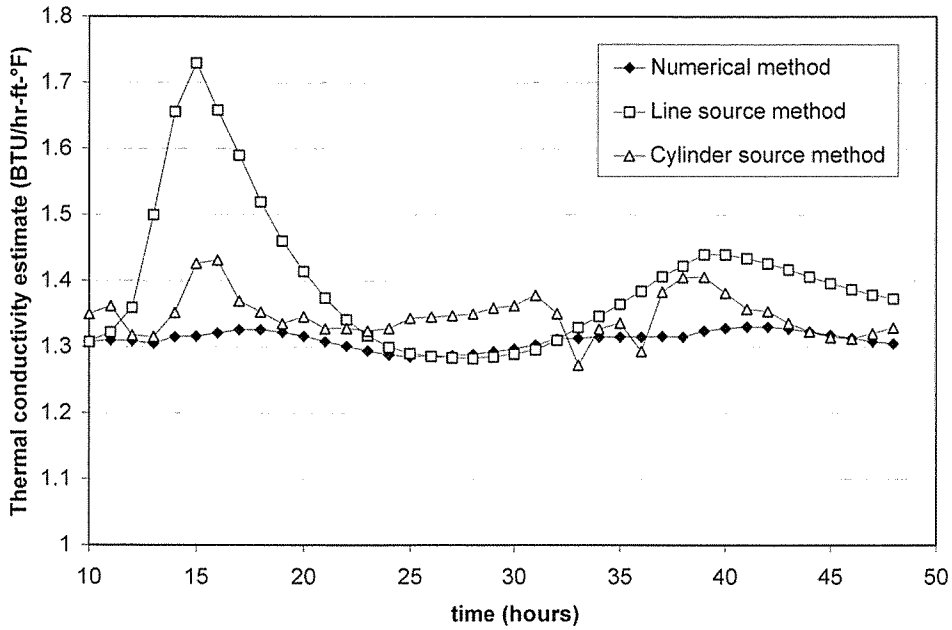

Fig. 3.14. Sequential thermal conductivity estimates from the data of Fig. 3.13.

3.3 CONCLUSIONS

The new method of determining soil thermal properties from in situ tests, which is based on a one-dimensional numerical heat transfer model, uses parameter estimation techniques to determine soil thermal conductivity and borehole resistance from field-collected data. Tests were needed to validate the method. For this purpose we used test data from an experimental test rig containing sand with a known thermal conductivity. We also conducted tests at schools in Lincoln, Nebraska, that already had one year of data from operating borefields.

For the test rig experiment at Oklahoma State University, in which a U-tube heat exchanger was placed in a medium with independently measured thermal properties, the model's predicted thermal conductivity showed excellent agreement with the measured value after 30 h. After 60 h the model predicted a slightly higher value of soil thermal conductivity (due perhaps to edge effects associated with the finite volume of the test rig), but the confidence interval still included the measured value.

For the tests in Lincoln, a total of three borehole heat exchangers were installed, two at Campbell Elementary School and one at Maxey Elementary School. The thermal conductivity test at Maxey agreed to within 4% with a separate thermal conductivity value for the site derived from one year of operating data from the borefield. The two tests at Campbell agreed with each other to within about 2%, but were lower than the values obtained for the Maxey site.

The borehole resistance values of the three heat exchangers were also estimated from the field data. The values measured were within the range of borehole resistances calculated for the grout materials, but because of uncertainty in shank spacing and the actual conductivity of the grout, we recommend that further experiments be performed to determine the reliability, accuracy, and repeatability of the borehole resistance measurements.

The thermal conductivity measurements from our method agree with the values obtained from the line source and cylinder source methods. This is to be expected because the power input was relatively stable during the course of the three experiments. Analysis of a separate data set showed that thermal conductivity estimates from the line source and cylinder source methods are significantly affected by variations in power input, while the thermal conductivity estimate from the method we have developed varied by only about 1% over the course of the experiment.

4. GPM SOFTWARE TUTORIAL

4.1 INTRODUCTION

This chapter provides an introduction to the features of the GPM program, including the options available in the main input menu and the information that is provided in the output window. Numerous illustrations show what the user will see on the computer screen.

4.2 MAIN MENU

The main menu, used for input, comes up automatically following an initial 3-s identification screen. A sample of the main page is shown in Fig. 4.1.

In the example shown in Fig. 4.1, the unit selection is the default value, which is the English unit system. The experimental data file and the output file are shown in the file name windows. The experimental data file name and/or the output file name can be manually typed into the appropriate file window.

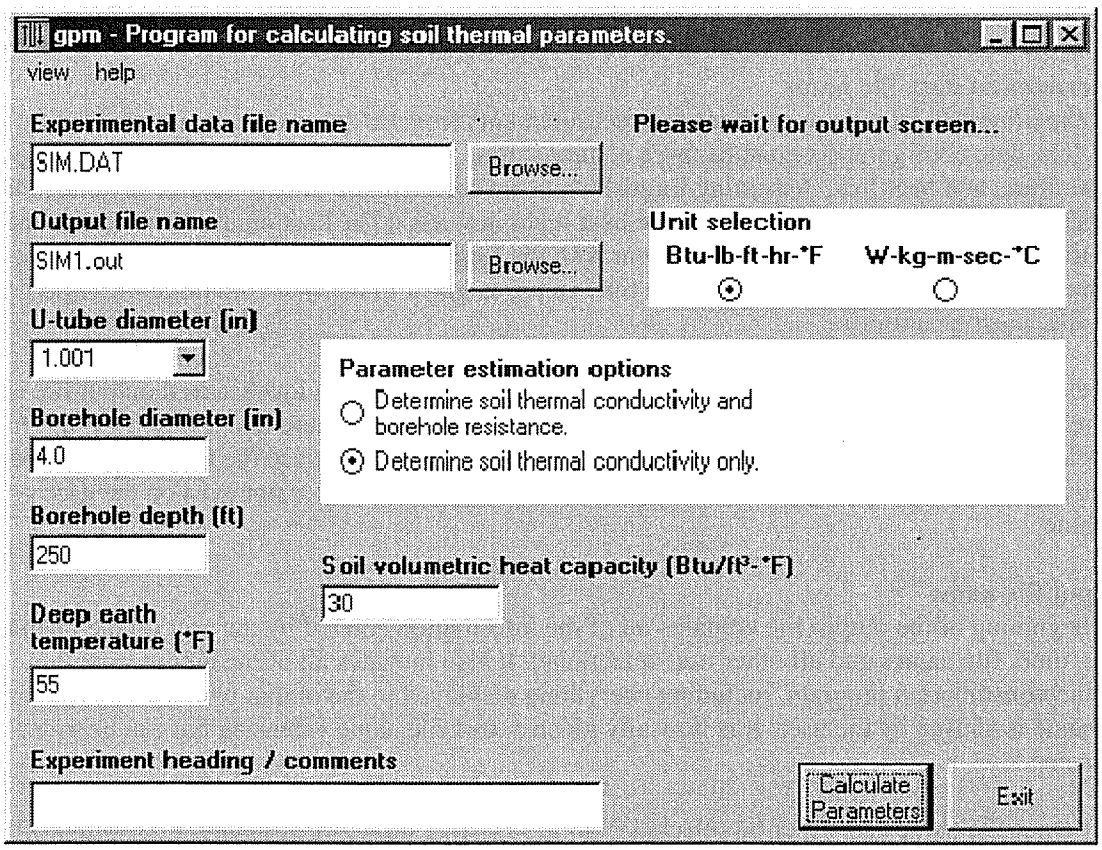

Fig. 4.1. The main data input screen in GPM.

Alternatively, the user can select the desired experimental data file or output file, as applicable, by using the **Browse** button. A file dialog box appears when **Browse** is selected. A sample of the file dialog box is shown Fig. 4.2. To make a selection, the user simply double-clicks the appropriate directory, if the desired directory is not already displayed. Following this, the user double-clicks the appropriate file name.

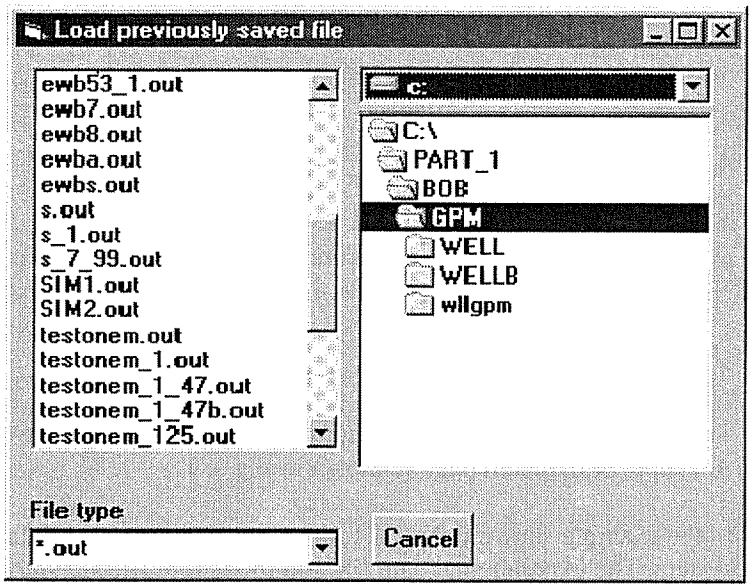

Fig. 4.2. A sample of the file dialog box.

If a disk drive other than the one containing gpm.exe is desired, this can be selected in the upper right hand corner of the file dialog box. Similarly, if an extension other than the default **.out** is desired, the appropriate selection can be made in the lower lefthand corner.

The following sections explain the input features on the main menu.

Experimental data file name

The experimental data file, containing the measurements from the borehole test, is provided by the user. The data configuration must be three columns: time, average (of the inlet and outlet) water temperature, and heat flux. Assuming English units are selected, the time should be in hours, the temperature in degrees Fahrenheit, and the heat input in watts. (The heat input unit is particularly important to note because it is not consistent with the English units.) The three columns may be separated by spaces or tab delimiters. The time steps, as given in the first column of the experimental data file, must be uniform.

The experimental data file name will be loaded automatically if a previously saved output file is used and reloaded. In this case, the user should verify the path listed to ensure that it is still valid. This is especially important when using a file from another user's machine, since the file may have been saved in a different directory structure on the other machine which does not exist on the user's machine.

Output file name

The beginning of the output file contains all of the information entered by the user on the main menu (date, time, file names and all other user selections). It also includes all of the output from the parameter estimation program, including everything displayed in the output window. The output data file name is chosen by the user. It is typically given a **.out** file name extension but can be saved under any name.

The output file name can either be selected from the existing directory structure, if an output file already exists, or entered manually. If it is desirable to save the file in a directory other than the GPM program directory, that directory should be entered in the **Output file name** window on the main menu.

If a new output file is being developed, the applicable experimental data file can be located using the **Browse** button next to the experimental data file line. Selecting this button automatically opens the file dialog box and allows the user to select the appropriate file by double-clicking on the desired directory and file name.

Unit selection

Although English units are by far the most common selection, and the system default, an option is provided for metric units. The user is automatically prompted to input data in the data boxes (described below) according to the unit system selected. The user must exercise care regardless of the system selected because the units designated for data input are not consistent; for example, data input in the English system uses both inches and feet. (See Fig. 4.1.)

Parameter estimation options

The main menu provides two options for analyzing borehole temperature data. These are found in the **Parameter estimation options** box. The available options are "Determine soil thermal conductivity and borehole resistance" (grout-soil model) and "Determine soil thermal conductivity" (homogeneous soil model).

Determine soil thermal conductivity and borehole resistance. This option provides two thermal parameter estimates. One parameter is soil thermal conductivity, and the other is borehole resistance. In addition, the deep earth temperature is estimated. For this model, the borehole grout is assumed to be a hollow cylinder of outer radius equal to the borehole radius and inner radius equal to the effective U-tube radius, r_i (Fig. 4.3). (For more discussion of r_i see the discussion of the U-tube diameter below.) Borehole resistance is simply the reciprocal of the heat transfer coefficient for a unit thickness of material, according to the equation

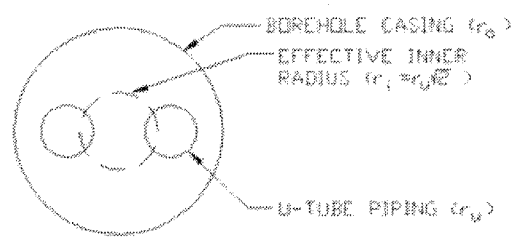

Fig. 4.3. Cross-sectional view of borehole showing dimensions.

$$\text{Borehole Resistance} = \frac{1}{2\pi k_g} \ln\left(\frac{r_0}{r_i}\right), \tag{4.1}$$

where r_o is the outer radius of the grout (i.e., the borehole radius), r_i is the effective inner radius (i.e., the actual outside U-tube radius multiplied by $\sqrt{2}$) and k_g is the thermal conductivity of the grout. The soil in this case is considered as a separate region, which is from r_o to a thermally large radius.

Determine soil thermal conductivity only. This is the simplest option and returns the soil thermal conductivity and the deep earth temperature, both with confidence regions. The model for this option assumes that the thermal properties of the grout are the same as that of the soil and lumps both materials into one region.

U-tube diameter

The U-tube diameter is the diameter of the inner tube of the borehole in the units shown on the caption for the data box. (English units are inches, and metric units are centimeters.) Standard sizes may be pulled down from a menu inside the data entry box. When standard U-tube diameters of ¾, 1, 1¼, 1½, or 2 in. are selected, these values are replaced automatically by the actual outer-diameter dimensions of 1.050, 1.315, 1.660, 1.900, or 2.375 in., respectively. One-half of these diameters is the

radius denoted r_u, which GPM then multiplies by $\sqrt{2}$ to simulate the inlet and outlet pipes. This gives the effective radius of $r_i = (2)^{1/2} r_u$.

Borehole diameter
The borehole diameter is the diameter of the outer borehole in the units (inches for English units) shown on the caption for the data box.

Borehole depth
The borehole depth is the depth of the borehole in the units (feet for English units) shown on the caption for the data box.

Deep earth temperature
The deep earth temperature normally entered is the starting temperature of the water exiting the borehole. It is an estimated quantity in GPM, but a realistic value should be entered here. Because it is used as prior information by the program, its value will have a small effect upon the final estimate of the deep earth temperature and a much smaller effect on the estimates of the thermal parameters.

Experiment heading/comments
This optional entry item allows the user to keep notes on particular items of interest having to do with an experiment or an analysis of an experiment. Since more than one analysis can be performed on one experiment, this can be used to distinguish between analyses.

Soil volumetric heat capacity
The default entry for soil volumetric heat capacity — 30 Btu/ft^3-°F in the English system — is typical for most soils. The range of volumetric heat capacity does not vary much around this. Even more important, the thermal conductivity estimates are relatively insensitive to the value of the volumetric heat capacity. If a value is known for a particular soil, however, it can be entered here. When a grout layer is included, a separate value for the grout can be entered.

View
A pull-down menu allows the user to choose whether or not the DOS shell program is to be viewed. The parameter estimation calculations are actually performed by a separate program called sub.exe that is called up by GPM. The user can view this program while it is running if desired. The default condition is to allow the program to run in a minimized state that is not visible to the user. A run-time indication is displayed in order to show the user that the calculations are being performed.

Calculate parameters
Once the Calculate Parameters button is selected, the parameter estimation calculations will begin. At this time, the output information is saved in the output file. If an output file of the name selected has already been saved by the user, a warning window will appear to ensure that the user realizes that the previous file will be overwritten. Following this, the calculations will begin, and the run-time indication will begin to display the number of seconds of run time. The output screen will automatically appear when the calculations are completed.

Exit
If the exit button is depressed, the program will stop. A user who wishes to continue using GPM will have to restart the program.

4.3 OUTPUT WINDOW

The output window contains all of the information contained in the output file. The window has four tab selection options, labeled **Tabular Output, Residuals, Sensitivity Coef.,** and **Sequential Est.** (see Fig. 4.4). The output presented in each of these windows is summarized below.

Tabular output
The tabular output window is the initial window that appears upon completion of the parameter estimation calculations. It provides the requested calculated parameter values in bold print at the top of a scrollable text screen. The remainder of the screen contains the contents of the entire output file, including input data, confidence regions, residuals, sequential parameter estimates, and sensitivity coefficients.

Residual plot
The residual plot is a graphical plot of the residuals vs time. The residuals are defined as the measured temperature values minus the calculated temperatures from the mathematical model. A plot of the residuals is valuable because this graph can be examined for a characteristic signature. Ideally, the residual graph should be purely random, reflecting random temperature measurement errors.

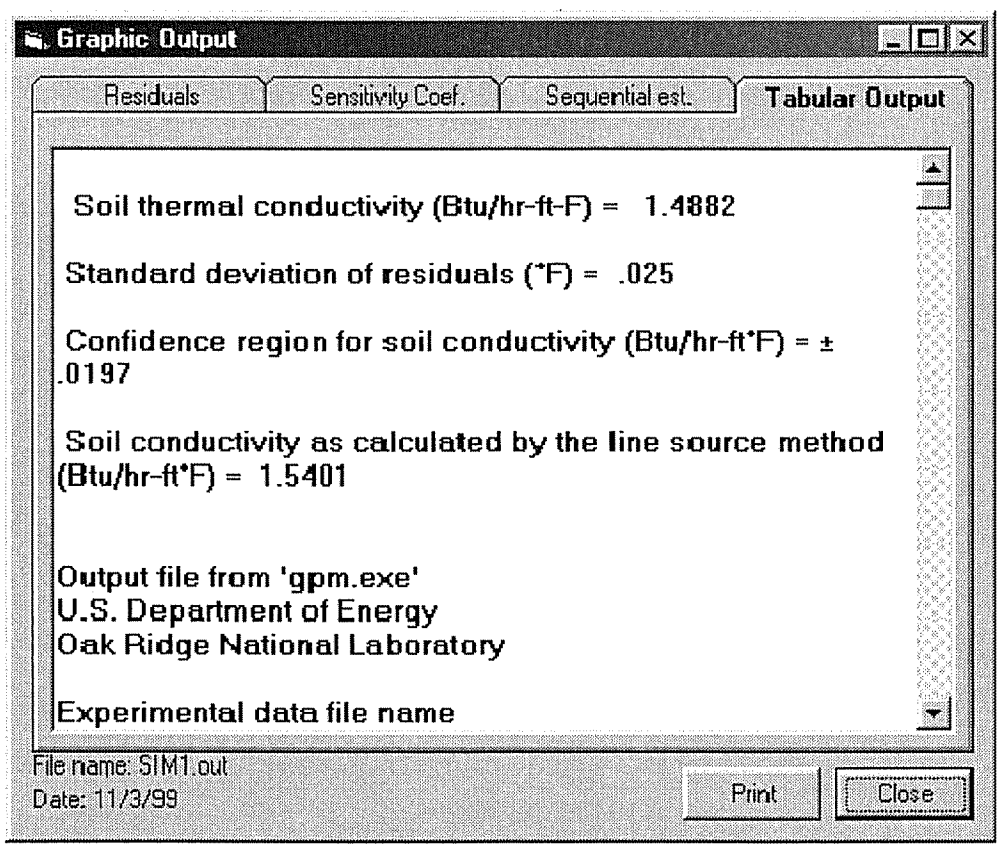

Fig. 4.4. The GPM output window. This screen, showing tabular output, is the output window that appears first.

Sensitivity coefficient plot
The sensitivity coefficient plot is a graphical representation of the modified sensitivity coefficients as functions of time. There are as many sensitivity coefficients as there are thermal parameters to be estimated. The sensitivity coefficient of the deep earth temperature is simply a constant with time and is not shown. The modified sensitivity coefficient for the soil conductivity is the soil conductivity multiplied by the partial derivative of the calculated temperature at r_i with respect to the soil conductivity. It has units of temperature and can be compared with the temperature rise.

Sequential parameter plot
The sequential parameter plot is a graphical representation of the sequential parameters as functions of time. There are as many sequential parameters to be plotted as there are thermal conductivities to be estimated. The sequential values are the estimated parameters using the experimental data only up to the corresponding time of the individual sequential parameter value. In a satisfactory analysis the sequential parameter estimates should be nearly constant for the last half of the duration of the experiment. If there is even a small drift upward or downward, an imperfection in the model or inaccuracies in the data (or both) are indicated.

Any of the above screens can be printed on the default printer for the machine in use simply by selecting the **Print** button. When printed, the data or plots appear as they do on the screen except that the tabs and buttons are not shown.

5. CONCLUSIONS

A new method has been developed for the calculation of effective soil formation thermal properties from short-term in situ field tests. The model underlying the method is one-dimensional radial heat conduction in a composite medium; the conduction problem is discretized using finite difference techniques and solved using the Crank-Nicolson scheme. The new method has been incorporated into The Geothermal Properties Measurement (GPM) model, a stand-alone computer program for the Windows 95/98 operating system.

In a short-term in situ field test, water is heated at a measured rate and pumped through a U-tube heat exchanger. The measurement technique we have developed requires interval data on the heat input to the heat exchanger and the average temperature of the water in the heat exchanger. The field-measured heat input is used to drive the numerical heat-transfer model of the soil and grout. The temperature at the centerline of the numerical model is compared to the field-monitored average water temperature, and the thermal properties of the model (deep earth temperature, thermal conductivity and thermal diffusivity of both the soil and the grout, etc.) are varied until the model's predictions match the field-monitored average water temperatures in a least-squares sense. All of these calculations are carried out by the software, which then reports the thermal properties and an estimate of their accuracy given the accuracy of the data.

The new method offers several advantages over the line source and cylinder source methods currently used to analyze data from short-term in situ field tests. First, unlike the line and cylinder source methods, the accuracy of our numerical method is not affected by short-term variations in power input to the heat exchanger. Second, our numerical method is more accurate at early times, and therefore does not require early data to be discarded, as do the line and cylinder source methods. Finally, unlike the simple curve-fitting techniques used with the line and cylinder source methods, our method provides a qualitative estimate of the accuracy of the thermal properties it reports.

The GPM software has been validated with tests on a dedicated thermal conductivity test rig and with data from field tests carried out in Lincoln, Nebraska.

6. REFERENCES

Alifanov, O. M. 1994. *Inverse Heat Transfer Problems.* New York: Springer-Verlag.

Austin, W. A. 1998. "Development of an In-Situ System for Measuring Ground Thermal Properties." M.S. thesis, Oklahoma State University.

Bard, Y. 1974. *Nonlinear Parameter Estimation.* New York: Academic Press.

Beck, J. V. 1999. User's Manual for IHCP1D: Program for Calculating Surface Flux from Transient Temperatures inside Solids. Okemos, Mich.: Beck Engineering Consultants Co.

Beck, J. V., and K. J. Arnold. 1977. *Parameter Estimation in Science and Engineering.* New York: John Wiley.

Beck, J. V., B. Blackwell, and C. R. St. Clair. 1985. *Inverse Heat Conduction: Ill-Posed Problems.* New York: John Wiley.

Beck, J. V., K. D. Cole, A. Haji-Sheikh, and B. Litkouhi. 1992. *Heat Conduction Using Green's Functions.* Washington, D.C.: Hemisphere Publishing Co.

Beck, J. V., and J. A. Shonder. 1998. "A Parameter Estimation Technique for Determining Soil Thermal Properties in the Design of Heat Exchangers for Geothermal Heat Pumps." In *Proceedings of the ASME Heat Transfer Division,* 3:221–40.

Bevington, P. R. 1969. *Data Reduction and Error Analysis for the Physical Sciences.* New York: McGraw-Hill.

Bose, J. E., J. D. Parker, and F. C. McQuiston. 1985. *Design/Data Manual for Closed-Loop Ground-Coupled Heat Pump Systems.* Atlanta: American Society of Heating, Refrigerating and Air-conditioning Engineers.

Carslaw, H. S., and J. C. Jaeger. 1947. *Conduction of Heat in Solids.* Oxford: Claremore Press.

Deerman, J. D., and S. P. Kavanaugh. 1991. "Simulation of Vertical U-Tube Ground-Coupled Heat Pump Systems Using the Cylindrical Heat Source Solution." *ASHRAE Transactions* 97, Pt. 1: 287–95.

Draper, N. R., and H. Smith. 1966. *Applied Regression Analysis.* New York: John Wiley.

Eskilson, P. 1987. *Thermal Analysis of Heat Extraction Boreholes.* Lund, Sweden: Dept. of Mathematical Physics, University of Lund.

Hellstrom, G. 1991. *Ground Heat Storage.* Lund, Sweden: Dept. of Mathematical Physics, University of Lund.

Ingersoll, L. R., O. J. Zobel, and A. C. Ingersoll. 1954. *Heat Conduction with Engineering, Geological and Other Applications.* New York: McGraw-Hill.

Kavanaugh, S., and K. Rafferty, K. 1997. *Ground-Source Heat Pumps: Design of Geothermal Systems for Commercial and Institutional Buildings.* Atlanta: American Society of Heating, Refrigerating and Air-conditioning Engineers.

Morgensen, P. 1983. "Fluid to Duct Wall Heat Transfer in Duct System Heat Storages." In *Proceedings of the International Conference on Subsurface Heat Storage in Theory and Practice,* Swedish Council for Building Research, June 6–8.

Rottmayer, S., W. A. Beckmann, and J. W. Mitchell. 1997. "Simulation of a Single Vertical U-Tube Ground Heat Exchanger in an Infinite Medium." *ASHRAE Transactions* 103, Pt. 2: 651–59.

Shonder, J. A., and J. V. Beck. 1999. "Determining Effective Soil Formation Thermal Properties from Field Data Using a Parameter Estimation Technique." *ASHRAE Transactions* 105, Pt. 1: 458–66.

Spitler, J. D. 1996. "Borehole Resistance Calculator." Excel spreadsheet distributed with GLHEPROWin. Available from the International Ground Source Heat Pump Association (IGSHPA), Stillwater, Oklahoma. See http://www.igshpa.okstate.edu/Publications/Catalog/1998/Software.html.

DISTRIBUTION

Internal

1. R. N. Baugh
2. V. D. Baxter
3. M. A. Brown
4. J. M. Campbell
5. J. E. Christian
6. G. E. Courville
7. P. D. Fairchild
8. S. K. Fischer
9. P. J. Hughes
10. J. Mike MacDonald
11. M. G. Madgett
12. M. M. Martin
13. M. A. Martin
14. C. I. Moser
15. T. R. Sharp
16. J. A. Shonder
17. J. J. Tomlinson
18. Laboratory Records – RC
19. Central Research Library

19–20. Laboratory Records – OSTI

External

21. James Adams, President, Energy Systems Group, 101 Plaza East Blvd., Suite 320, Evansville, IN 47715-2804
22. Michael Albertson, Global Logic, Inc., 4508 Blackberry Run, Oklahoma City , OK 73112
23. Phil Albertson, Charles Machine Works/Ditch Witch, P.O. Box 735, Perry, OK 73077
24. Howard Alderson, Alderson Engineering, Inc., 1588 Heather Road, Huntingdon Valley, PA 19006
25. Charlene Aleman, The Trane Company, P.O. Box 7916, Waco, TX 75714
26. Tom R. Amerman, EnLink Geoenergy Services, Inc., 16430 Park Ten Place, Suite 600, Houston, TX 77084
27. David Ames, Jr., Vice President, Virginia Energy Services, 3200 West Moore Street, Richmond, VA 23230
28. David Austin, SRS Corp., 5625 Dillard Drive, #101, Cary, NC 27511
29. Charles Aycock, Duke Engineering and Services Inc., P.O. Box 1004, Charlotte, NC 28201-1004
30. Byron H. Bakenhus, Lincoln Electric System, 11th and "O" Streets, P.O. Box 80869, Lincoln, NE 68501
31. Michael Baker, Baker, EMS, Inc., 304 W. DuVall Street, Philadelphia, PA 19144
32. Tom Balster, Alliant Energy, P.O. Box 769, Dubuque, IA 52004-0769
33. John Barlean, Northwest Rural Public Power District, P.O. Box 249, Hay Springs, NE 69347
34. Kevin Barrett, P.O. Box 270983, Oklahoma City, OK 73137-0983
35. Daniel C. Baublis, Energy Alternatives, LLC, 20 Jason Lane, Mansfield, MA 01048
36. Greg Behe, Allegheny Power, 800 Cabin Hill Dr., Greensburg, PA 15601
37. Rodger Bekooy, CBG Consulting Engineers, 6650 SW Redwood Lane, Suite 355, Portland, OR 97224
38. Kevin Bellamy, Constellation Energy Source, Inc., 111 Market Place, Suite 530, Baltimore, MD 21202
39. Jeannette Bennion, General Manager, e.three, P.O. Box 30069, Reno, NV 89520-3069

40. Scott J. Benson, Lincoln Electric System, 11th & "O" Streets, P.O. Box 80869, Lincoln, NE 68501
41. Gary T. Bergeron, Kelso-Regen Associates, 6709 Kingston Pike, Knoxville, TN 37919
42. Mark Berman, Davis Energy Group, 123 C Street, Davis, CA 95616
43. Peter Bibb, Alaska Electric Light and Power, 5601 Tongsgard Court, Juneau, AK 99801
44. Kenneth Black, Entergy Systems & Services, 2410 Shrewbury Run, Collierville, TN 38017
45. John Bleem, P.E. Platte River Power Authority, 2000 E. Horsetooth Road, Fort Collins, CO 80525-5721
46. R. Gordon Bloomquist, Washington State University Energy Program, 925 Plum Street SE, Bldg., #4, P.O. Box 43165, Olympia, WA 98504
47. Roger Bohon, ENCAP Systems Inc., 1202 Franklin Road, Roanoke, VA 24016
48. Suzette Bollinger, Fall River Rural Electric, 714 Main Street, P.O. Box 830, Ashton, ID 83420
49. James Bose, Oklahoma State University, Engineering Technology, 294 Cordell South, Stillwater, OK 74078
50. Jos Bouma, IEA Heat Pump Centre, Swentiboldstraat 1, Box 17, 6137 AE Sittard, Netherlands
51. Jerry Brandom, UtilCorp United, Inc., 20 West 9th Street, Kansas City, MO 64105
52. David Branson, Compliance Services Group, Inc., 7619 University Avenue, Unit 2A, Lubbock, TX 79423-2126
53. Harry J. Braud, 13519 Bluff Road, Geismar, LA 70734
54. Richard Bremer, EnerShop Inc., 1616 Woodall Rogers Freeway, Dallas, TX 75202
55. Jim Brennan, Ancoma, Inc., 395 Maple Street, Rochester, NY 14611
56. Charles R. Brockmeier, Brockmeier Consulting Engineers, 1304 Olympic Blvd., Santa Monica, CA 90404
57. Robert Brown, ClimateMaster, 4060 N. 100 West, Markle, IN 46770
58. Wyatt Brown, AEP Energy Services, One Riverside Plaza, Columbus, OH 43215-2355
59. Jerry Bruce, Kentucky Utilities Co., 1 Quality Street, Lexington, KY 40507
60. Tim Burke, HydroDelta Corp., 10205 Gravois, St. Louis, MO 63123
61. Kathy Butcher, National Ground Water Association, 601 Dempsey Road, Westerville, OH 43081
62. Ralph Cadwallader, Loop-Tech International, 607 Highway 19, Huntsville, TX 77340
63. Douglas Cane, Caneta Research, Inc., Suite 102, Bldg. 2, 7145 W. Credit Avenue, Mississauga, Ontario L5N 6J7 Canada
64. Steven Carlson, CDH Energy Corp., P.O. Box 641, Cazenovia, NY 13035
65. Millard E. Carr, Energy Management Solutions, Inc., 9213 Hidden Creek Drive, Great Falls, VA 22066
66. Ken Carrara, Long Island Power Authority, 131 South Hoffman Lane, Central Islip, NY 11749
67. Beatriz Casals, Casals & Associates, Crystal Park Three, Suite 814, 2331 Crystal Drive, Arlington, VA 22202
68. Frank Cassidy, Energis Resources Inc., 499 Thornall Street, Edison, NJ 08837
69. Ron Castle, American Geothermal, 1037 Old Salem Road, Murfreesboro, TN 37129
70. John Castelvecchi, Evantage, a Division of Virginia Power, 6300 Kennedy Court, Mechanicsville, VA 23111-5037
71. Jim Caughran, ProSolutions, 3101 Carlisle Street, Columbia, SC 29205
72. T. L. Cavines, Evantage, 5000 Dominion Boulevard, Glen Allen, VA 23060
73. Roger Chamberlain, Riley Engineering, Inc., N. 1501 Howard Street, Spokane, WA 99201
74. Harold Chappell, CEO, IllumElex Corporation, 2925 Huntleigh Dr., Suite 104, P.O. Box 10461, Raleigh, NC 27604
75. Heath Chelisvig, Oklahoma State University, IGSHPA, 490 Cordell South, Stillwater, OK 74078
76. Joe Childress, Childress Engineering Corp., 393-D NE 33rd Ter., Kansas City, MO 64117
77. Randy P. Christenson, Karges & Associates, 1611 W. County Road B, St. Paul, MN 55113-4053
78. Tim Clemons, Executive Vice President of Business Development, Custom Energy, L.L.C., 9217 Cody, Overland Park, KS 66214

79. Greg Collins, PEPCO Services Inc., 2000 K Street NW, Suite 750, Washington, DC 20006
80. Tony Cooper, WaterFurnace International, Inc., 9000 Conservation Way, Fort Wayne, IN 46809
81. Glen Coury, Coury and Associates, Inc., P.O. Box 666, Wheatridge, CO 80034
82. Russell L. Cowan, Moon Lake Electric Assn., P.O. Box 278, 188 W. 200 North, Roosevelt, UT 84066
83. David H. Crabtree, American Electric Power Service Corp., 1 Riverside Plaza, Columbus, OH 43215-2373
84. Don Creyts, Advanced Geothermal Technologies, P.O. Box 511, Reading, PA 19607
85. Gary Crooks, Avista Advantage Inc., P.O. Box 3727, Spokane, WA 99220
86. D. Brooks Cross, D. Brooks Cross Chartered Co., 8415 Old Marlboro Pike, Upper Marlboro, MD 20772
87. Peter Crossman, Boral Energy, Level 5, 35 Waymouth Street, Adelaide, SA, Australia 5000, GPO Box 1199, Adelaide, SA, Australia 5001
88. Bill Dakin, Davis Energy Group, 123 C Street, Davis, CA 95616
89. Jim Damiani, Climate Master, 7300 SW 44th Street, P.O. Box 25788, Oklahoma City, OK 73125
90. Michael Dandrea, AYP Capital, 800 Cabin Hill Dr., Greensburg, PA 15601
91. Mary Darden, KU Solutions Corp., One Quality Street, Lexington, KY 40507
92. Mike Davis, OG&E Electric Services, P.O. Box 321, Oklahoma City, OK 73101-0321
93. Tim Day, GPU, 300 Madison Avenue, Morristown, NJ 07962
94. Diana L. Dean, P.E., Colorado Springs Utilities, 6 North Tejon Street, MC 146, P.O. Box 1103, Colorado Springs, CO 80947-1546
95. Willard G. DeGraaf, Mich Con, 500 Griswold Street, Detroit, MI 48226
96. Sam Dellario, Government Projects Director, Viron Corporation, 216 NW Platte Valley Drive, Riverside, MO 64150
97. Victor DeMarco, DeMarco Energy Systems of America, Inc., P.O. Box 201057, Austin, TX 78720
98. Karen Den Braven, University of Idaho, Mechanical Engineering Department, Moscow, ID 83844-0902
99. Alan F. Destribats, Xenergy Inc., 3 Burlington Woods, Burlington, MA 01803-4543
100. Leonard DeVanna, COM/Energy Enterprises Inc., One Main Street, Cambridge, MA 02142
101. Joseph J. DeVirgilio, Jr., Central Hudson Gas & Electric, 284 South Avenue, Poughkeepsie, NY 12601
102. Jack Dienna, Member Services Manager, Geothermal Heat Pump Consortium, Inc., 701 Pennsylvania Avenue NW, Washington, DC 20004-2696
103. John Dilliplane, Preferred Products Group, 214 W. State Street, Trenton, NJ 08608-1002
104. David Dinse, Tennessee Valley Authority, 1101 Market Street, Chattanooga, TN 37402-2801
105. Shawn Dion, Rose Technology Group, Inc., Suite 300, Bldg. 5, Foster Plaza, 651 Holiday Drive, Pittsburgh, PA 15220-2740
106. Gino Di Rezze, Groundheat Systems International, 15450 Yonge Street, Aurora, Ontario L4G-1P2, Canada
107. Bob Donaldson, Carolina Power and Light Co., 7001 Pinecrest Road, Raleigh, NC 27613
108. Robert Dooley, R. J. Dooley & Associates, 1 Rock Garden Way, Poughkeepsie, NY 12603
109. Floyd Dooris, Central Hudson Enterprises Corp., 110 Main Street, Poughkeepsie, NY 12601
110. Rose Dowdy, Geo Air, 2201 Lou Ellen, Houston, TX 77018
111. Homer D. Duff, ENCAP Systems, Inc., 1202 Franklin Road, Roanoke, VA 24016
112. Bob Dupuis, Strategic Resource Solutions, 1099 Gum Branch Road, Jacksonville, NC 28540
113. Dave Dutton, McElroy Manufacturing, Inc., P.O. Box 580550, Tulsa, OK 74158-0550
114. Oree Dyes, Energy Environment Education, 2000 L Street NW, Suite 2000, Washington, DC 20036
115. Robert F. Edwards, Enova Energy, Inc., P.O. Box 126211, San Diego, CA 92130
116. Ray Ehmer, HL&P Energy Services Inc., P.O. Box 4300, Houston, TX 77210-4300

117. Larry Eitelman, FHP Manufacturing, 565 S. Hudson Avenue, Tulsa, OK 74112
118. Lance Elberling, Pacific Gas & Electric, 123 Mission Street, P.O. Box 770000, San Francisco, CA 94177
119. Dan Ellis, ClimateMaster, 7300 SW 44th Street, P.O. Box 25788, Oklahoma City, OK 73125
120. William Ely, Heat Controller, 1900 Wellworth Avenue, Jackson, MI 49203
121. Roger K. Emmons, Process Improvement Engineering, 12768 Chilicothe, Chesterland, OH 44026
122. Gary J. Epstein, Energy & Resource Solutions, 45 Wingate Street, Haverhill, MA 01830
123. Stephen R. Etsler, NIPSCO Energy Services Inc., 5265 Holman Avenue, Hammond, IN 46320
124. Kris Ewbank, Ewbank & Associates, P.O. Box 148, Fairview, OK 73737
125. Jeffery M. Fang, National Renewable Energy Laboratory, 409 12th Street SW, Suite 710, Washington, DC 20024
126. Mark Farnsworth, Chimney Rock Public Power Div., P.O. Box 608, 805 W. 8th Street, Bayard, NE 69334
127. Barry Ferguson, E+ Engineering, Inc., 1502 Kiehl Avenue, Suite A, Sherwood, AR 72120
128. Ronald S. Feuerbach, Alvine and Associates, Inc., 1102 Douglas on the Mall, Omaha, NE 68102
129. Craig Fischbach, Mammoth, Inc., 101 West 82nd Street, Chaska, MN 55318
130. Bradley J. Fisher, Friedman Fisher Associates, 22 Aviation Road, Albany, NY 12205
131. Philip Fleischman, Evantage, a Division of Virginia Power, 6300 Kennedy Court, Mechanicsville, VA 23111-5037
132. William S. Fleming, Jacwill Services, Inc., 4571 East Lake Road, Cazenovia, NY 13035
133. J. Kevin Fletcher, Southern Company Services, Inc., 333 Piedmont Avenue, Atlanta, GA 30308
134. Frederick G. Florian, BGE Energy Projects & Services Inc., 7225 Windsor Blvd., Baltimore, MD 21244
135. David Foreman, Foreman Architects Engineer., P.O. Box 189, Zelienople, PA 16063
136. Ray Fortuna, U.S. Department of Energy, 1000 Independence Avenue, S.W., Code 342, Washington, DC 20585
137. Gustav Foster, Jr., 1240 S. Spring Road, Vineland, NJ 08361
138. D. J. Frandsen, Jr., T.U. Electric, Energy Plaza, 1601 Bryan Street, Suite 22052, Dallas, TX 75201-3411
139. Lisa Frantzle, Arthur D. Little, Inc., Acorn Park, Cambridge, MA 02140-2390
140. J. Phillip Frazier, Plum Street Enterprises Inc., 507 Plum Street, Syracuse, NY 13204
141. William Gang, The Enron Team, 12647 Alcosta Blvd., Suite 500, San Ramon, CA 94583
142. Robert Gardner, The Trane Company, 1804 Inspiration Lane SE, Huntsville, AL 35801-1149
143. William R. Gee, Jr., Potomac Electric Power Co., 1500 Pennsylvania Avenue NW, Washington, DC 20068-0001
144. W. Geoghegan, WEDGCO Engineering, 1375 Piccard Dr., Ste. 1, Rockville, MD 20850-4311
145. John D. Geyer, JG&A, Inc., P.O. Box 87490, 11914 NE 18th Street, Vancouver, WA 98687
146. David C. Gill, Director of Sales, Siebe Environmental Controls, 1354 Clifford Avenue, Loves Park, IL 61111
147. Robert L. Gluck, Alliance to Save Energy, 1200 18th Street NW, Suite 900, Washington, DC 20036
148. Jared Goetz, Detroit Edison Co., 2000 2nd Avenue, 314 W., Detroit, MI 48226
149. Fred Goldstein, T. C. Technologies, 1605 Lake Las Vegas Parkway, Henderson, NV 89011
150. H. Lawrence Goldstein, National Renewable Energy Laboratory, 409 12th Street SW, Suite 710, Washington, DC 20024-2125
151. Richard Gordon, Gordon Associates, 508 S.W. Jefferson, Corvallis, OR 97333
152. Joy Grand, New York State PTA, 3778 Dunhill Road, Wantagh, NY
153. David Graves, Eau Claire Electric Cooperative, 8214 Highway 12, P.O. Box 368, Fall Creek, WI 54742
154. William Greelis, Cinergy Solutions Inc., 139 East Fourth Street, Cincinnati, OH 45202

155. Bruce Green, National Renewable Energy Laboratory, 1617 Cole Boulevard, Golden, CO 80401-3393
156. Dan Grover, GPU Advanced Resources Inc., 2675 Morgantown Road Suite GH2-3300, Reading, PA 19607
157. James Guertin, HEC Energy Services, Inc., 24 Prime Parkway, Natick, MA
158. Anita Gursahani, LLNL-Custom Power Group & Eng., 7000 East Avenue, P.O. Box 808, L-604, Livermore, CA 94551
159. Joseph Gustin, Mid-America Energy Resources Inc., One Monument Circle, Indianapolis, IN 46206-6161
160. Richard Hackner, Energy Center of Wisconsin, 595 Science Drive, Madison, WI 53711-1060
161. Brian Haggart, The Environmental Group, 7300 Southwest 44th Street, Oklahoma City, OK 73125
162. Bob Halvorson, HVAC Reps Inc., 6210 Pioneer Trail, P.O. Box 362, Loretta, MN 55357
163. Don Hamilton, Carolina Power & Light Co., 1099 Gum Branch Road, Jacksonville, NC 28540
164. John Haney, FPL Energy Services, Inc., 700 Universe Blvd., Juno Beach, FL 33408-2657
165. Lilli Hardin, Hardin Technologies, P.O. Box 53770, Indianapolis, IN 46253-0770
166. Bob Harvey, Navy Public Work Center, Oceana Naval Air Station, Virginia Beach, VA 23460
167. Scott Heath, Chotawhatchee Electric Coop., 1350 W. Baldwin Avenue, DeFuniak Springs, FL 32433
168. Kenneth Hedges, FirstEnergy, 6200 Oak Tree Blvd., MS Ind-349, Independence, OH 44131
169. William Heil, All Energy Marketing Company, LLC95 Sawyer Road, Waltham, MA 02154
170. Harold Heiss, 6860 Kilt Court, Worthington, OH 43085-2129
171. John K. Helbling, Alliant, 200 First Street SE, P.O. Box 351, Cedar Rapids, IA 52406
172. Hugh Henderson, CDH Energy Corp., P.O. Box 641, Cazeovia, NY 13035-0641
173. Bill Herbert, Energy Assets, Inc., 2003 Renaissance Boulevard, King of Prussia, PA 19406
174. Lisa S. Hermann, Butler REC, Inc., 3888 Stillwell-Beckett Road, Oxford, OH 45056
175. Michael E. Hill, CES/Way International, Inc., 2500 City West Boulevard, Suite 1800, Houston, TX 77042
176. Carl Hiller, Manager, Geothermal Heat Pumps and Water Heating, EPRI, 3412 Hillview Avenue, P.O. 10412, Palo Alto, CA 94303
177. Ernest C. Hoelzer, Navy Public Works Center, Code 332 Energy Management Branch, 9742 Maryland Avenue, Norfolk, VA 23511-3095
178. Kent Hoffman, Schlenger/Pitz & Associates, Inc., 15 W. Aylesbury Road, Timonium, MD 21093
179. Ron Hohlfeld, Dow Chemical Co., 1691 Swede Road, Midland, MI 48674
180. Michiel Hoogstede, Puget Sound Energy Services, 26317 Ansell Road NW, Poulsbo, WA 98370
181. Alfred D. Hopp, Alvine and Associates, 1102 Douglas on the Mall, Omaha, NE 68102
182. Phyllis Hoshino, Natural Resources Canada, 580 Booth Street, 17th Floor, Ottawa, Ontario K1A 0E4, Canada
183. Robert E. Hough, Syracuse Energy, 159 Dwight Park Drive, Syracuse, NY 13209
184. Kent Hudson, Knowledge Builders Inc., 111 East Main Street, Coats, NC 27521
185. Steve Hudson, Hydro-Temp Corp., P.O. Box 566, Pocahontas, AR 72455
186. Gary Jacobs, Hydro Pump Co., 3616 S. 138th Street, Omaha, NE 68144
187. Gregory S. Jarosinski, Constellation Energy Source, 111 Market Place, Suite 530, Baltimore, MD 21202
188. Michael D. Jenkinson, Environmental Solutions Spec., 5909 NW Expressway, Suite 4, Oklahoma City, OK 73132
189. Myles L. Jensen, Nodak Electric Coop., 400 32nd Avenue South, P.O. Box 13000, Grand Forks, ND 58208
190. Keith Johnson, Central Maine Power Co., 162 Canco Road, Portland, ME 04103
191. Ric Johnson, Empire Energy Services, P.O. Box 127, Joplin, MO 64802
192. Brad Jones, BRJ Engineering, 78 County Road, Simsbury, CT 06070

193. John Judge, CONECO Corporation, 280 Summer Street, Boston, MA 02210
194. Phil Kairis, Dakota Energy Altenatives, 4300 220th Street W., Farmington, MN 55024-9583
195. Michael Kapps, T. C. Technologies, 1605 Lake Las Vegas Parkway, Henderson, NV 89011
196. Larry Kaufman, Detroit Edison Co., 2000 2nd Avenue, 318 WCB, Detroit, MI 48226
197. Steve Kavanaugh, University of Alabama, Box 870276, 290 Hardaway Hall, Tuscaloosa, AL 35487-0276
198. Joseph G. Keller, Lockheed Martin Idaho Technologies Co., P.O. Box 1625, Idaho Falls, ID 83415
199. Daniel J. Kendra, Foreman Architects Engineering, 525 New Castle Street, Zelienople, PA 16063
200. Timothy C. Kessler, Hill Engineering & Contracting, 105 Quince Dr., Telford, PA 18969
201. John Kierzkowski, Spectrum Energy Services Corp., Two North Ninth Street, Allentown, PA 18101
202. Erbin B. Keith, CES/Way International, Inc., 2500 City West Boulevard, Suite 1800, Houston, TX 77042
203. Thomas R. Killebrew, Clarke Electric Coop., Inc., P.O. Box 161, 1103 North Main, Osceola, IA 50213
204. Jerry L. Kinzie, Spectrum Engineers, PC, 325 Mountain Avenue SW, Roanoke, VA 24016
205. James S. Kish, Engineering Elements, Inc., 4950 E. 345th Street , Willoughby, OH 44094
206. Kathleen Kraft, ClimateMaster, 7300 Southwest 44th Street, Oklahoma City, OK 73179
207. David Kramka, Johnson Controls Inc., 2400 Kilgust Road, Madison, WI 53713
208. Kent Kufner, WaterFurnace International, Inc., 9000 Conservation Way, Fort Wayne, IN 46809
209. Jackie LaMarsh, Enertran, Inc., 15082 Ilderton Road, RR#3, Ilderton, Ontario N0M 2A0, Canada
210. Rich Landy, Entergy Integrated Solutions Inc., 4740 Shelby Drive, #105, Memphis, TN 38118
211. Jack Lann, Lann Mechanical Contractors, 1604 Westchester Street, Shreveport, LA 71119
212. Rod Larson, PEPCO Services Inc., 2000 K Street NW, Suite 750, Washington, DC 20006
213. Robert P. Lewis, II, Director, Major Energy Projects, BGE Energy Project & Services, Inc., 7225 Windsor Boulevard, Baltimore, MD 21244
214. Tom Lewis, Centerprise Inc., One Main Street, #600, Minneapolis, MN 55414
215. Brett G. Lichtenthaler, Siebe Environmental Controls, 10 Industrial Avenue, Mahwah, NJ
216. Edward T. Liston, President, EUA Cogenex Corporation, Boott Mills South, 100 Foot of John Street, Lowell, MA 01852
217. Lee Loomis, Rochester Gas and Electric Corp., 89 East Avenue, Rochester, NY 14649-0001
218. Nance Lovvorn, Alabama Power / Southern Company, 600 N. 18th Street, P.O. Box 2641, Birmingham, AL 35291
219. Robert L. Lyles, Jr., Core Care, Inc., 923 Bywater Road, Annapolis, MD 21401
220. Kimberly A. Magrini, National Renewable Energy Laboratory, 1617 Cole Boulevard, Golden, CO 80401-3393
221. John Mahoney, President, Viron Energy Services, 216 NW Platte Valley Drive, Riverside, MO 64150
222. Robert Mancini, Mancini, Saldan Associates Ltd., 5468 Dundas Street West, Etobicoke, Ontario M9B 6E3, Canada
223. John Manning, Phoenix Geothermal Services, P.O. Box 3, Skaneateles, NY 13152
224. Robert Marshall, Plumas-Sierra Rural Electric, 73233 Highway 70, Suite A, Portola, CA 96122
225. Cheryl C. Mattson, Northeast Utilities, P.O. Box 270, Hartford, CT 06141
226. Edward Mayberry, PEPCO Services, Inc., 2000 K. Street NW, #750, Washington, DC 20006
227. Paul McConvey, Virginia Power and Light, 2700 Cromwell Road, Norfolk, VA 23509-2406
228. Kevin B. McCray, National Ground Water Association, 601 Dempsey Road, Westerville, OH 43081
229. Michael McGrath, Edison Electric Institute, 701 Pennsylvania Avenue NW, Washington, DC 20004-2696

230. Nancy McMann, National Rural Electric Cooperative Association, 4301 Wilson Boulevard, EP11-255, Arlington, VA 22203
231. Cam McNeil, CSLM Associates, 3 Sandwell Crescente, Kanata, Ontario K2K1V2, Canada
232. Tom Meanwell, Firelands Electric Coop., One Energy Place, New London, OH 44851
233. Lisa Meline, Meline Engineering, P.O. Box 276665, Sacramento, CA 95827
234. David J. Meyer, Pathfinder Engineers LLP, 3300 Monroe Avenue, Suite 306, Rochester, NY 14618
235. Frank A. Migneco, GPU Energy, 300 Madison Avenue, P.O. Box 1911, Morristown, NJ 07962
236. Phillip M. Mikulsky, WPS Energy Services Inc., 677 Baeten Road, Green Bay, WI 54304
237. Gary Miles, Sr., Conectiv Services, Inc., P.O. Box 2167, West Chester, PA 19380-0092
238. Leland Mink, Idaho Water Resources Research Institute, Morrill Hall, Room 201, University of Idaho, Moscow, ID 83844
239. Thomas W. Mitchell, President, Co-Energy Group, Suite N136, 1050 E. Flamingo Road, Las Vegas, NV 89119
240. Dave Molin, The Trane Company, 4831 White Bear Parkway, Saint Paul, MN 55110
241. Kevin Mooney, BGE Energy Projects & Services, Inc., 7225 Windsor Boulevard, Baltimore, MD 21244
242. Spencer Morasch, GPU Energy, 525 Main Street, Allenhurst, NJ 07711
243. Edward Morofsky, Public Works and Government Services, Canada, 2968 Southmore Drive, Ottawa, Ontario K1V 6Z3, Canada
244. Richard Morra, Commonwealth Electric Co., 157 Cordaville Road, Southboro, MA 01772
245. Duncan Morrison, Combined Energies Inc., 41 Anthony Avenue, Augusta, ME 04330
246. Mitchell V. Morse, Precision Power, Inc., 165 Skiff Street, Hamden, CT 06517
247. Andrew Moyad, PEPCO Services, Inc., 2000 K Street NW, #750, Washington, DC 20006
248. Tatiana Muessel, Office of Federal Energy Management Programs, U.S. Department of Energy, EE 090, 1000 Independence Avenue SW, Washington, DC 20585
249. David Munn, Southwest HEC, 1232 E. Broadway Road, Tempe, AZ 85282-1509
250. Edward Murphy, Western Massachusetts Electric Co., P.O. Box 2010, West Springfield, MA 01090-2010
251. Jay Murphy, K & M Shillingford, Inc., 5004 E. Archer, Tulsa, OK 74115-4833
252. Michael Murphy, WaterFurnace International, 9000 Conservation Way, Fort Wayne, IN 46809
253. William Murphy, University of Kentucky, Agricultural Engineering Department, 128 Agricultural Engineering Bldg., Lexington, KY 40546-0276
254. William E. Muston, TXU Services, 1601 Bryan Street, Dallas, TX 75201
255. Jerry Neese, Georgia Power Co., 241 Ralph McGill Boulevard NE, Bin 10210, Atlanta, GA 30308
256. Howard Newton, The Trane Co., P.O. Box 7916, Waco, TX 76714
257. Richard Niess, Gilbert & Associates, Gloucester Point Office Plaza, Suite D, 1811 G Washington Memorial Highway, Gloucester Point, VA 23062
258. Mark Nofi, EnerVision, P.O. Box 1349, Tucker, GA 30085
259. Gregory Nolan, Nolan Heating & Air, Inc., 301 N. Mill Street, Colfax, WA 99111
260. Darin Nutter, University of Arkansas, Department of Mechanical Engineering, Mechanical Engineering Building, Fayetteville, AR 72701
261. Thomas O'Day, Today Associates, Inc., 500 S. Salina Street, Syracuse, NY 13202
262. Paul Ogle, Knowledge Builders Inc., 111 East Main Street, Coats, NC 27521
263. Arthur N. Olson, American Electric Power, One Riverside Plaza, 27th Floor, Columbus, OH 43215-6642
264. Thomas O'Neill, Energy Source, Inc., 111 Market Place, Suite 530, Baltimore, MD 21202
265. Carl Orio, Water & Energy Systems Corp. — ClimateMaster, 100 Maple Avenue, Atkinson, NH 03811-2245
266. Greg Orman, Custom Energy LLC, 6409 City West Parkway, Eden Prairie, MN 55344

267. Dale W. Osborn, Distributed Generation Systems, Inc., 2334 Pine Tree, Evergreen, CO 80439
268. Thomas Ott, Palisades Energy Services Inc., One Blue Hill Plaza, Pearl River, NJ 10965
269. Susie Overholser, Econar Energy Systems Corp., 19230 Evans Street, Elk River, MN 55330
270. G. Ronald Owens, Mid America Drilling Equipment, Inc., 5802 SW 6th Place, Ocala, FL 34474
271. Fred Paepke, Bard Manufacturing Co., 1914 Randolph Dr., P.O. Box 607, Bryan, OH 43506
272. Steve Paiewonsky, HydroDelta Corporation, 5 Pocono Heights, E. Stroudsburg, PA 18301
273. John Parker, Brandt Engineering, 2840 Plol Parkway, Suite 200, Midlothian, VA 23113
274. Steven A. Parker, Pacific Northwest National Laboratory, 902 Battelle Boulevard, P.O. Box 999, Richland WA 99352
275. Joe Parsons, ECR Technologies, P.O. Box 3271, Lakeland, FL 33802
276. Robert Payne, Director, Federal Energy Services, DukeSolutions, Inc., 230 South Tryon Street, Suite 400, Charlotte, NC 28202
277. Stephen Pazian, Edison Source, 13191 Crossroads Parkway N, #405, City of Industry, CA 91746
278. Don Penn, Don Penn Consulting Engineers, 1600 Airport Freeway, Suite 508, Bedford, TX 76022
279. George Penn, Global Energy Options, 4634 Bonner Lane, Madison, WI 53704-1327
280. Gary Phetteplace, U.S. Army Cold Regions Lab, 72 Lyme Road, Hanover, NH 03755-1290
281. Tony Pierce, Souther California Edison, 6042 N. Irwindale Avenue, Suite B, Irwindale, CA 91702
282. Charles Peterson, Virginia Energy Services, 3000 West Moore Street, Richmond, VA 23230
283. David Pleasants, James M. Pleasants Co, Inc., 603 Diamond Hill Court, P.O. Box 16706, Greensboro, NC 27416
284. Thomas W. Philbin, President, HEC Energy Corporation, 24 Prime Parkway, Natick, MA 01760
285. David Phillips, Geo-Energy, 1916 Spiller Way, Ft. Walton Beach, FL 32547
286. Mirek Piechowski, Earth Energy Systems, P.O. Box 240, Golden Square, Bendigo, Victoria 3555 Australia
287. R. A. (Tony) Pierce, Southern California Edison, 300 North Lone Hill Avenue, San Dimas, CA 91773
288. Marion Pinckley, Pinckley Engineering, Inc., 233 W. Broadway, Suite 530, Louisville, KY 40202
289. Lew Pratsch, U.S. Department of Energy, 1000 Independence Avenue SW, Code 342, Washington, DC 20585
290. Terry Proffer, Sound Geothermal, R2233 East Main, Montrose, CO 81401
291. Pete Prydybasz, HydroDelta Corporation, 2352A Wentzel Road, RD 2, Mohnton, PA 19540
292. Kevin Rafferty, GEO Heat Center, Oregon Institute of Technology, 3201 Campus Drive, Klamath Falls, OR 97601
293. John Ramill, Bosek Gibson and Associates, 508 West Fletcher Avenue, Tampa, FL 33612
294. Kenneth Randazzo, Detroit Edison Co., 2000 Second Avenue, Detroit, MI 48226-1203
295. Chitra Ranganathan, Spectrum Engineers, PC, 325 Mountain Avenue SW, Roanoke, VA 24016
296. Phil Rawlings, The Rawlings Company, 2308 Watchill Drive, Greenville, TX 75402-6444
297. Karl R. Rebago, CH2M Hill, 6060 S. Willow Drive, Greenwood Village, CO 80111-5142
298. Philips Reese, Conectiv Service, P.O. Box 6066, Newark, DE 19714-6066
299. Michael W. Reid, PG&E Energy Services, 507 Canyon Boulevard, Suite 200, Boulder, CO 80302
300. Charles Remund, South Dakota State University, 210B CEH, ME Dept., Brookings, SD 57007
301. Tim Reynolds, Balzhiser & Hubbard Engineering, 975 Lincoln Street, Eugene, OR 97401
302. Scott W. Rhoads, Parfitt/Ling, 101 Fraser Street, State College, PA 16801
303. Randy Richgruber, Minnesota Power Company, 30 W Superior Street, Duluth, MN 55802
304. Ronald A. Robertson, Energy Assets, Inc., 2003 Renaissance Boulevard, King of Prussia, PA 19406
305. James T. Rodriguez, James T. Rodriguez Consulting, 15600 San Pedro Avenue, Suite 209, San Antonio, TX 78232

306. Harry Roth, New Jersey Heat Pump Council, 20000 Horizon Way, Suite 200, Mt. Laurel, NJ 08054
307. Frank Rotondi, MP Energy Services Company, 40 East Broadway, Butte, MT 59701
308. Michael J. Rubala, Southern Maryland Electric Coop., 15065 Burnt Store Road, P.O. Box 1937, Hughesville, MD 20837-1937
309. Harvey Sachs, Geothermal Heat Pump Consortium, 701 Pennsylvania Avenue, 3rd Floor, Washington, DC 20004-2696
310. Stephen P. Sain, Sain Engineering Associates Inc., 2820 Columbiana Road, Suite 100, Birmingham, AL 35216
311. Douglas Sattler, Energy Assets, 2003 Renaissance Boulevard, King of Prussia, PA 19406
312. Nancy Schibonski, Northern States Power–MN, 414 Nicollet Mall, RS-55, Minneapolis, MN 55401
313. Phil Schoen, Geo-Enterprises, P.O. Box 691453, Tulsa, OK 74169-1453
314. Richard E. Schonbachler, Baltimore Gas & Electric Co., 7130 Rutherford Road, Baltimore, MD 21244
315. Robert Schultz, Illinova Energy Partners, 1420 Kensington Road, #305, Oak Brook, IL 60521
316. Bill Scribner, OG&E, 101 N. Robinson, Oklahoma City, OK 73102
317. Vicki Severson, Otter Tail Power Co., 215 South Cascade, P.O. Box 496, Fergus Falls, MN 56537
318. Christopher S. Sharpe, Duke Power Company, 526 S. Church Street, P.O. Box 1006, Charlotte, NC 28201-1006
319. Rita Sharpe, Westar Energy, 818 Kansas Avenue, Topeka, KS 66612
320. Karen R. Sheehe, Clark Electrical/Mechanical, 3109 Lincoln Highway East, Paradise, PA 17562
321. Craig Shepard, QST Energy, Inc., 300 Hamilton Boulevard, #300, Peoria, IL 61602
322. William Shivly, CMS Marketing Services and Trading, One Jackson Square, Suite 1060, Jackson, MI 49201
323. Samar Sibani, Concordia University, 3460 Peel, #302, Montreal, Quebec H3A 2M1, Canada
324. Rogelio Sigrist, Sol-R-Tek, Priv. 7A sur 4512, Col. G. Pasto, Puebla, Mexico 72420
325. A. Glenn Simpson, PEPCO Services Inc., 2000 K Street NW, #750, Washington, DC 20006-7276
326. Jitendra Singh, J & P Engineers, 14 Kory Drive, Kendall Park, NJ 08824-1608
327. Allan Skouby, GeoPro, Inc., 1444 Rogers Court, Allen, TX 75013
328. Cary Smith, Sound Geothermal, Route 3, Box 3010, Roosevelt, UT 84066
329. Chris Smith, FHP Manufacturing, 601 NW 65th Court, Ft. Lauderdale, FL 33309
330. David Smith, Malcolm Pirnie, Inc., P.O. Box 1938, Buffalo, NY 14219
331. Donald O. Smith, Energy Masters Corp., 9101 W. 110th Street, #200, Overland Park, KS 66210
332. Geoffrey Smith, Bechtel Corp., 45 Fremont Street, San Francisco, CA 94105
333. Marvin Smith, Oklahoma State University, GHP Research, 499 Cordell South, Stillwater, OK 74078
334. Peter Smith, Sear-Brown Group, 85 Metro Park, Rochester, NY 14623
335. Robert Smith, Commonwealth Edison, 1919 Swift Road, Oak Brook, IL 60521
336. Bruce A. Soukup, Soukup Heating & Air Conditioning, 1404-179th Street, East Moline, IL 61244
337. Scott D. Souza, Noresco, 111 Speen Street, Framingham, MA 01701
338. Jeffrey Spitler, Oklahoma State University, School of Mechanical & Aerospace Engineering, Engineering North 218, Stillwater, OK 74078
339. Bruce Stanley, Omaha Public Power District, 444 S. 16th Street Mall, 2E/EP2, Omaha, NE 68102-2247
340. Ray Starling, HEI Power Corporation, P.O. Box 3160, Honolulu, HI 96802
341. David Stone, Larson Design Group, 1000 Commerce Park Drive, PO Box 487, Williamsport, PA 17703-0487

342. Jeffery C. Stott, S. L. King & Associates, 34 Peachtree Street NW, One Park Tower, Suite 1, Atlanta, GA 30303
343. R. B. Stotz, Stotz, Sebring & Townsend, 433 Harrison Ave, Panama City, FL 32401
344. Ted Striplin, McElroy Manufacturing, Inc., 833 N. Fulton, Tulsa, OK 74115
345. Deborah Sumlin, PEPCO Services, Inc., 1900 Pennsylvania Avenue NW, Suite K307, Washington, DC 20068
346. Stephen Sunderhauf, Potomac Electric Power Co., 1900 Pennsylvania Avenue NW, Room 842, Washington, DC 20006
347. S. Lynn Sutcliffe, SYCOM Enterprises, First Floor, 27 Worlds Fair Drive, Somerset, NJ 08873
348. Bob Sweitzer, BGE Energy Projects & Services, Inc., 7225 Windsor Boulevard, Baltimore, MD 21207
349. Joseph Swift, Northeast Utilities System, 107 Selden Street, Berlin, CT 06037
350. Keith Swilley, Gulf Power Co., 1230 E. 15th Street, P.O. Box 2448, Panama City, FL 32405
351. Carl E. Syversen, Syversen Engineering Assoc., 7029, Northview Drive, Urbandale, IA 50322
352. Frederick Tate, Long Island Power Authority, 510 Park Avenue, West Babylon, NY 11704-7900
353. Jeff Tawney, Aqua Cal, 2737 24th Street N., St. Petersburg, FL 33713
354. Buck Taylor, Connecticut Light and Power, 107 Selden Street, Berlin, CT 06037
355. Scott Terrell, Truckee Donner PUD, P.O. Box 309, Truckee, CA 96160
356. Tom Thomas, Dixie Escalante REA, 145 W. Brigham Road, St. George, UT 84790
357. Jeff Thornton, Thermal Energy System Specialists, 5610 Medical Circle, Suite 31, Madison, WI 53719
358. Karen Thrasher, Townsend Engineering, P.O. Box 23526, Chattanooga, TN 37422
359. James Tobia, GPU Energy, 2800 Pottsville Pike, Reading, PA 19640-0001
360. Terry E. Townsend, T. E. Townsend Engineering, Inc., 5611 Ringgold Road, Suite 200, P.O. Box 23526, Chattanooga, TN 37422
361. Louis Torbett, Torbett Engineering, Inc., 4137 S. Harvard, Suite B, Tulsa, OK 74135
362. Jon Trabert, Nebraska Public Power District, P.O. Box 499, Columbus, NE 68602
363. B. N. Tripathi P.E., CES/Way International Inc., 5308 Ashbrook, Houston, TX 77081
364. Darryl Tveitbakk, Northern Municipal Power Agency, 123 North Main Avenue, P.O. Box 528, Thief River Falls, MN 56701-0528
365. Garry M. Upton, Decision Analyst, Inc., 604 Avenue H East, Arlington, TX 76011-3100
366. Mutch Usera, Black Hills Power & Light Co., P.O. Box 1400, Rapid City, SD 57709
367. Gary Valli, Allegheny Power, 800 Cabin Hill Drive, Greensburg, PA 15601
368. Roger VanLaningh, Lincoln Electric System, P.O. Box 80869, Lincoln, NE 68508
369. Eileen Vieira, Ancoma, Inc., 395 Maple Street, Rochester, NY 14611
370. Bruce Vincent, Sacramento Municipal Utility District, 6301 South Street, Sacramento, CA 95817-1899
371. Georg Volkel, Coventry Holdings, Ltd., 1/4 19-23-27 WPM, Inglis, Manitoba R0J 0X0, Canada
372. Greg Volkman, Jaed Corp., #6 Village Square, Smyrna, DE 19977
373. Dave Wagner, Kansas City Power and Light Co., P.O. Box 418679, Kansas City, MO 64141
374. Joel Wagner, Southwest Energy Solutions Inc., P.O. Box 711, Tucson, AZ 85702
375. James Walters, Rochester Public Utilities, 4000 East River Road, NE, Rochester, MN 55906
376. Art Warner, St. Joseph Light & Power Co., 520 Francis Street, P.O. Box 998, St. Joseph, MO 64502
377. Kellogg Warner, Xenergy, Inc., 3 Burlington Woods, Burlington, MA 01803-4543
378. Tom Warner, Warner Systems, 4808 Meadow Wood Drive, Waco, TX 76710
379. Gregory Warren, PEPCO Services, Inc., 2000 K Street NW, Suite 750, Washington, DC 20006
380. Rod Weaver, Addison Products, 7050 Overland Road, Orlando, FL 32810
381. Steven M. Wegman, South Dakota Public Utilities Commission, State Capitol, Pierre, SD 57501-5070
382. John Welch, Secure Energy Inc., One Northshore Center, Pittsburgh, PA 15212

383. Steve White, Phillips Driscopipe, Inc., P.O. Box 83-3866, Richardson, TX 75080
384. Bob Williamson, Addison Products Co., 7050 Overland Road, Orlando, FL 32810
385. Daniel Willis, Red River Valley REA, P.O. Box 220, 1003 Memorial Drive, Marietta, OK 73448
386. Kerry R. Wilson CEM CLEP, Evantage, One James River Plaza, 7th Floor, 701 E. Cary Street, Richmond, VA 23219
387. Buddy Winslow, Winslow Pump and Well, Inc., P.O. Box 521, Hollywood, MD 20636
388. Philip J. Wirdzek, U.S. Environmental Protection Agency, Office of Administration and Resource Management, 401 M Street SW, Washington, DC 20460
389. Brian Wolka, Jackson County REMC, 274 E. Base Road, P.O. Box K, Brownstown, IN 47220
390. Stephen Woods, BGE Energy Projects & Services, Inc., 7725 Windsor Boulevard, Baltimore, MD 21244
391. Barry K. Worthington, United States Energy Associates, 1300 Pennsylvania Avenue NW, Suite 550, Mailbox 142, Washington, DC 20004-3022
392. Richard W. Wright, America Thru Wall Manufacturing Corp., 59 BC Remington Boulevard, Ronkonkoma, NY 11779
393. Dave H. Yohanna, Ryerson Polytechnic University, 22 Jeffcoat Dr., Etoblooke, Ontario M9W-3B4, Canada
394. Grenville Yuill, University of Nebraska–Omaha, Department of Architectural Engineering, 6001 Dodge Street, Omaha, NE 68182
395. Shawn YunSheng Xu, Department of Mechanical & Aerospace Engineering, University of Missouri–Columbia, Columbia, MO 65211
396. Steven J. Zach, Nebraska Public Power District, 1414 15th Street, P.O. Box 499, Columbus, NE 68602-0499
397. Paul Zeigler, NCSBCS, 505 Huntmar Park Drive, #210, Herndon, VA 20170
398. Richard Zimbone, CONECO Corp., 280 Summer Street, Boston, MA 02210